Multigrid Hirsch-Fye quantum Monte Carlo method for dynamical mean-field theory

Nils Blümer, Univ. Mainz

Outline

Introduction: Hubbard model, DMFT, HF-QMC

Efficiency of QMC DMFT solvers

Unbiased Green functions and spectra from HF-QMC

Multigrid Hirsch-Fye quantum Monte Carlo algorithm

Spectral weight transfer at the Mott transition

Summary and outlook

Introduction

Hubbard model

(i) Single band: $\hat{H} = \sum_{(i,j),\sigma} t_{ij} \left(\hat{c}^{\dagger}_{i\sigma} \hat{c}_{j\sigma} + \text{h.c.}\right) + U \sum_{i} \hat{n}_{i\uparrow} \hat{n}_{i\downarrow}$

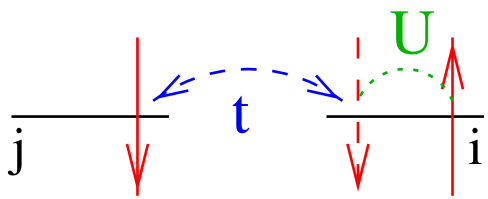

Captures important strong-correlation phenomena: Mott metal-insulator transition, (anti-) ferromagnetism, heavy fermions, high-T_c superconductivity (?), . . .

Few parameters: interaction U/W, temperature T/W, filling n, dispersion $\epsilon_{\boldsymbol{k}}$

Introduction

Hubbard model

(i) Single band: $\hat{H} = \sum_{(i,j),\sigma} t_{ij} \left(\hat{c}^{\dagger}_{i\sigma} \hat{c}_{j\sigma} + \text{h.c.}\right) + U \sum_{i} \hat{n}_{i\uparrow} \hat{n}_{i\downarrow}$

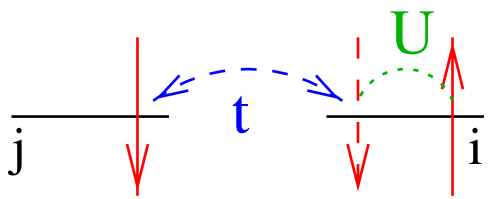

Captures important strong-correlation phenomena: Mott metal-insulator transition, (anti-) ferromagnetism, heavy fermions, high-T_c superconductivity (?), . . .

Few parameters: interaction U/W, temperature T/W, filling n, dispersion $\epsilon_{\boldsymbol{k}}$

(ii) Multi-band model, e.g., 2-band model with inequivalent bands:

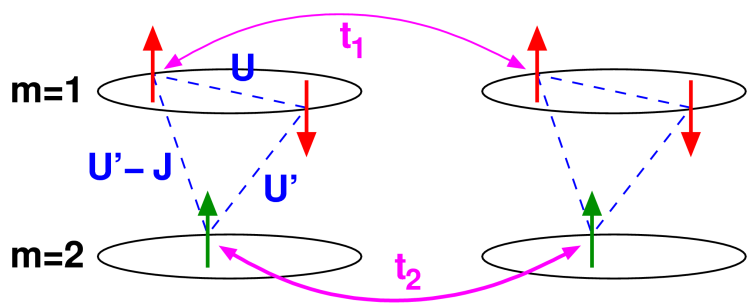

Introduction

Hubbard model

(i) Single band: $\hat{H} = \sum_{(i,j),\sigma} t_{ij} \left(\hat{c}^\dagger_{i\sigma} \hat{c}_{j\sigma} + \text{h.c.}\right) + U \sum_i \hat{n}_{i\uparrow} \hat{n}_{i\downarrow}$

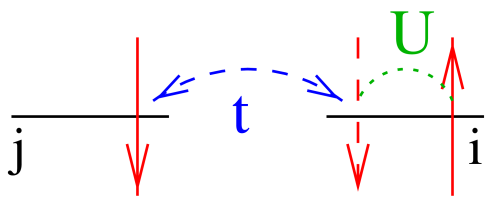

Captures important strong-correlation phenomena: Mott metal-insulator transition, (anti-) ferromagnetism, heavy fermions, high-T_c superconductivity (?), . . .

Few parameters: interaction U/W, temperature T/W, filling n, dispersion $\epsilon_{\boldsymbol{k}}$

(ii) Multi-band model, e.g., 2-band model with inequivalent bands:

$$H = \sum_{m=1}^{2} \left[-\sum_{\langle ij \rangle \sigma} t_m \, c^\dagger_{im\sigma} c_{jm\sigma} + U \sum_i n_{im\uparrow} n_{im\downarrow} \right]$$

$$+ \sum_{i\sigma\sigma'} \left(U' - \delta_{\sigma\sigma'} J_z\right) n_{i1\sigma} \, n_{i2\sigma'}$$

$$+ \frac{1}{2} J_\perp \sum_{i\sigma} \left[c^\dagger_{i1\sigma} \left(c^\dagger_{i2\bar{\sigma}} c_{i1\bar{\sigma}} + c^\dagger_{i1\bar{\sigma}} c_{i2\bar{\sigma}} \right) c_{i2\sigma} + \text{h.c.} \right]$$

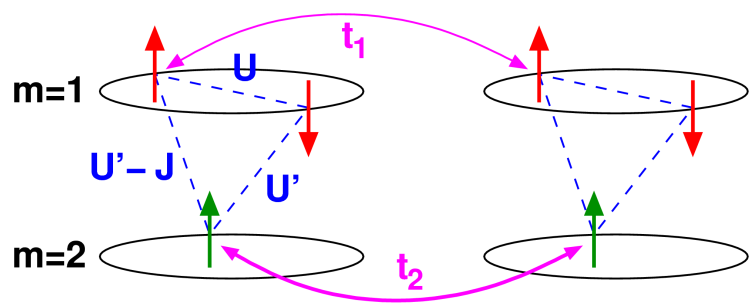

Introduction

Hubbard model

(i) Single band: $\hat{H} = \sum_{(i,j),\sigma} t_{ij} \left(\hat{c}^{\dagger}_{i\sigma} \hat{c}_{j\sigma} + \text{h.c.}\right) + U \sum_{i} \hat{n}_{i\uparrow} \hat{n}_{i\downarrow}$

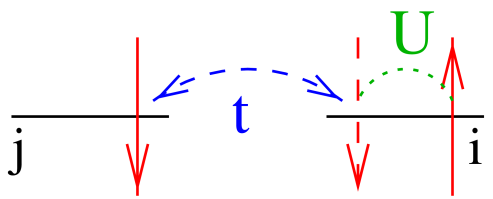

Captures important strong-correlation phenomena: Mott metal-insulator transition, (anti-) ferromagnetism, heavy fermions, high-T_c superconductivity (?), . . .

Few parameters: interaction U/W, temperature T/W, filling n, dispersion $\epsilon_{\boldsymbol{k}}$

(ii) Multi-band model, e.g., 2-band model with inequivalent bands:

$$H = \sum_{m=1}^{2} \left[-\sum_{\langle ij \rangle \sigma} t_m \, c^{\dagger}_{im\sigma} c_{jm\sigma} + U \sum_{i} n_{im\uparrow} n_{im\downarrow} \right]$$

$$+ \sum_{i\sigma\sigma'} \left(U' - \delta_{\sigma\sigma'} J_z\right) n_{i1\sigma} \, n_{i2\sigma'}$$

$$+ \frac{1}{2} J_{\perp} \sum_{i\sigma} \left[c^{\dagger}_{i1\sigma} \left(c^{\dagger}_{i2\bar{\sigma}} c_{i1\bar{\sigma}} + c^{\dagger}_{i1\bar{\sigma}} c_{i2\bar{\sigma}} \right) c_{i2\sigma} + \text{h.c.} \right]$$

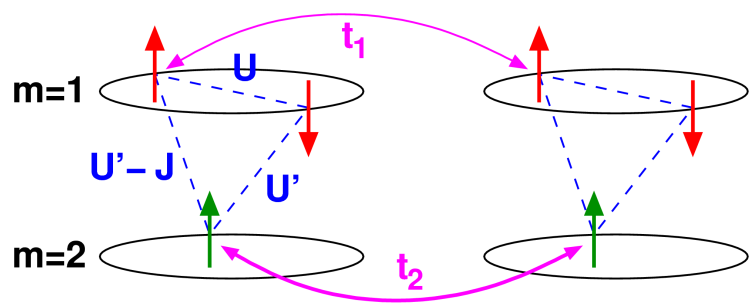

More complexity, more realistic: OSMT, spin+orbital order, LDA+DMFT, . . .

Approaches for Hubbard-type models

$$\hat{H} = \sum_{(i,j),\sigma} t_{ij} \left(\hat{c}^{\dagger}_{i\sigma} \hat{c}_{j\sigma} + \text{h.c.}\right) + U \sum_{i} \hat{n}_{i\uparrow} \hat{n}_{i\downarrow}$$

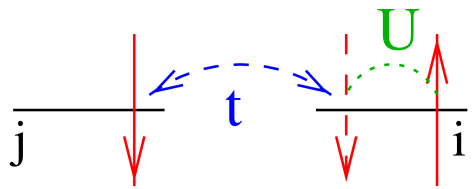

Perturbation theory

- $U \to 0$: Hartree-Fock
  2^{nd} order PT, . . .
- $t/U \to 0$ (for $n = 1$)
  $\rightsquigarrow$ Heisenberg model

finite clusters: ED, QMC

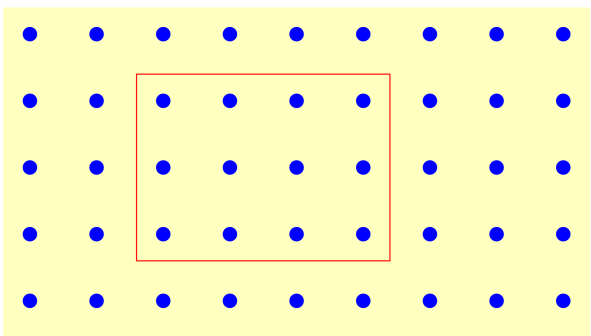

$d \to 1$: Bethe ansatz, DMRG

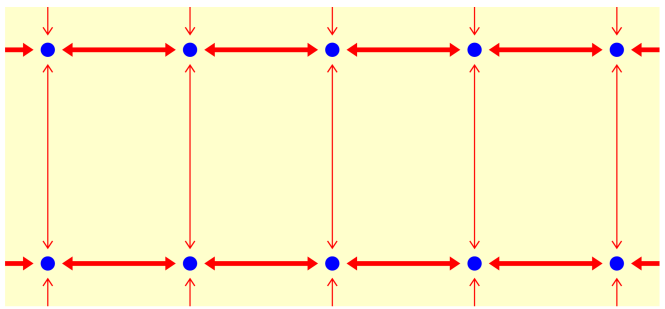

Approaches for Hubbard-type models

$$\hat{H} = \sum_{(i,j),\sigma} t_{ij} \left(\hat{c}^{\dagger}_{i\sigma} \hat{c}_{j\sigma} + \text{h.c.}\right) + U \sum_{i} \hat{n}_{i\uparrow} \hat{n}_{i\downarrow}$$

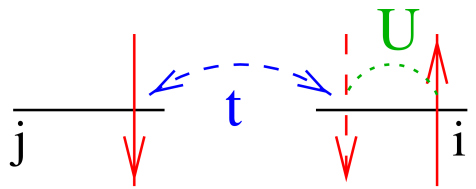

Perturbation theory

- $U \to 0$: Hartree-Fock
  2^{nd} order PT, . . .
- $t/U \to 0$ (for $n = 1$)
  $\rightsquigarrow$ Heisenberg model

finite clusters: ED, QMC

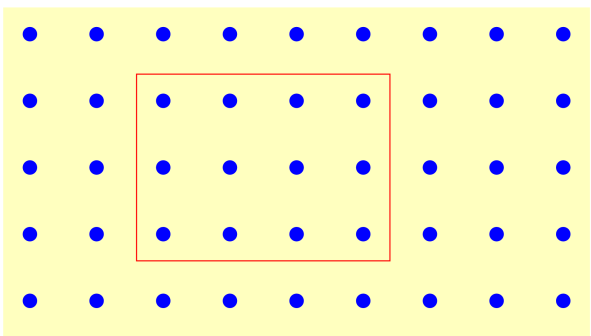

$d \to 1$: Bethe ansatz, DMRG

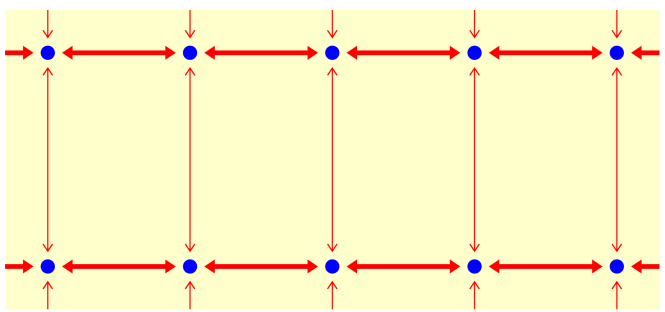

Dynamical mean-field theory (DMFT): local self-energy $\Sigma(\boldsymbol{k}, \omega) \equiv \Sigma(\omega)$

[Metzner, Vollhardt, PRL (1989), Georges, Kotliar, PRL (1992), Jarrell, PRL (1992)]

\+ non-perturbative $\rightsquigarrow$ valid at MIT

\+ dynamical on-site correlations preserved

\+ in thermodynamic limit

+/− exact for coordination $Z \to \infty$

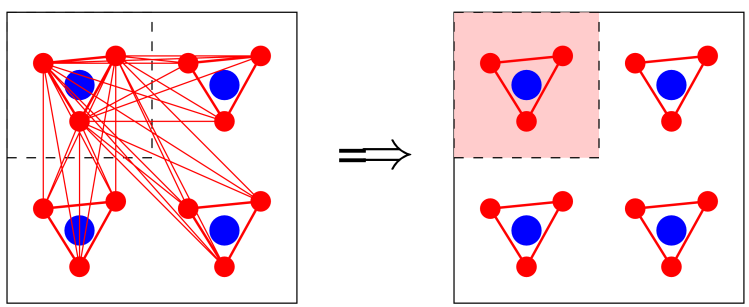

Iterative solution of DMFT equations

0. Initialize self-energy
1. Solve Dyson equation
2. Solve single impurity Anderson model (SIAM)

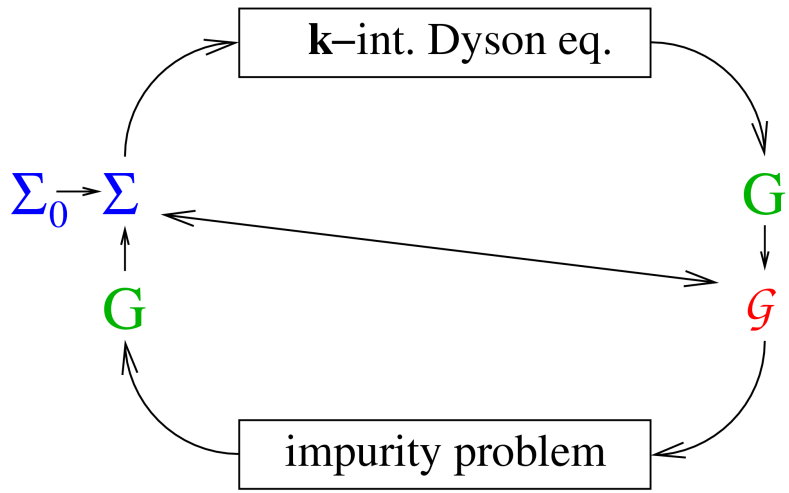

⟵ DOS / t_{ij} / $\varepsilon_{\nu \boldsymbol{k}}$

⟵ local interactions

Iterative solution of DMFT equations

0. Initialize self-energy
1. Solve Dyson equation
2. Solve single impurity Anderson model (SIAM)

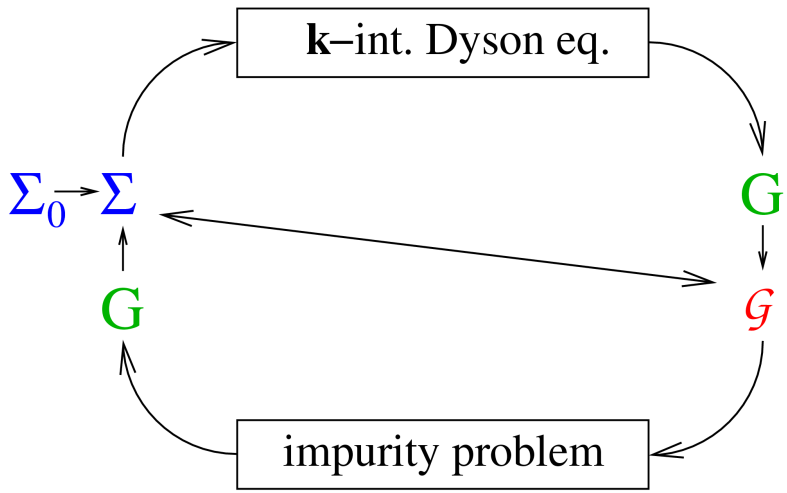

← DOS / t_{ij} / $\varepsilon_{\nu \boldsymbol{k}}$

← local interactions

Impurity solver:

- Iterative perturbation theory (IPT; not controlled)
- Quantum Monte Carlo (QMC)

Iterative solution of DMFT equations

0. Initialize self-energy
1. Solve Dyson equation
2. Solve single impurity Anderson model (SIAM)

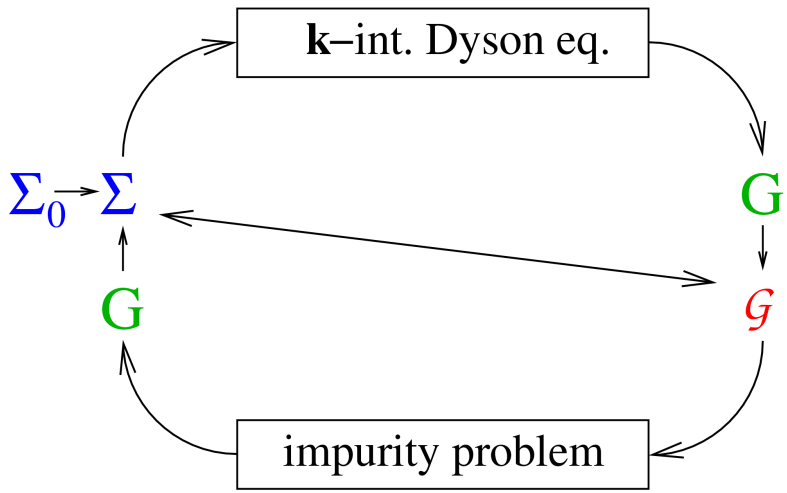

⟵ DOS / t_{ij} / $\varepsilon_{\nu \boldsymbol{k}}$

⟵ local interactions

Impurity solver:

- Iterative perturbation theory (IPT; not controlled)
- Quantum Monte Carlo (QMC)
- Exact diagonalization (ED; large finite-size errors)
- Numerical renormalization group (NRG; 1-2 bands)
- Density matrix renormalization group (DMRG)
- Self-energy functional theory (SFT) + ED

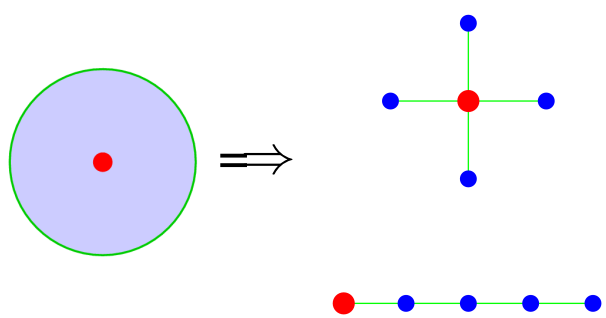

Auxiliary-field QMC algorithm [Hirsch, Fye (1986)]

Green function G in imaginary time (fermionic Grassmann variables ψ, ψ^*):

$$G_\sigma(\tau_2 - \tau_1) = \frac{1}{\mathcal{Z}} \int \mathcal{D}[\psi]\, \mathcal{D}[\psi^*]\ \psi_\sigma(\tau_1)\psi^*_\sigma(\tau_2)\ \exp\Big[\mathcal{A}_0 - U \sum_{\sigma\sigma'} \int_0^\beta d\tau\, \psi^*_\sigma \psi_\sigma \psi^*_{\sigma'} \psi_{\sigma'}\Big]$$

Auxiliary-field QMC algorithm [Hirsch, Fye (1986)]

Green function G in imaginary time (fermionic Grassmann variables ψ, ψ^*):

$$G_\sigma(\tau_2 - \tau_1) = \frac{1}{\mathcal{Z}} \int \mathcal{D}[\psi]\, \mathcal{D}[\psi^*]\ \psi_\sigma(\tau_1)\psi^*_\sigma(\tau_2)\ \exp\Big[\mathcal{A}_0 - U \sum_{\sigma\sigma'} \int_0^\beta d\tau\, \psi^*_\sigma \psi_\sigma \psi^*_{\sigma'} \psi_{\sigma'}\Big]$$

- Discretization $\beta = \Lambda\, \Delta\tau$,
- Trotter decoupling $e^{-\beta(\hat{T}+\hat{V})} = \lim_{\Lambda\to\infty} \left[e^{-\Delta\tau \hat{T}} e^{-\Delta\tau \hat{V}}\right]^\Lambda$

Auxiliary-field QMC algorithm [Hirsch, Fye (1986)]

Green function G in imaginary time (fermionic Grassmann variables ψ, ψ^*):

$$G_\sigma(\tau_2-\tau_1) = \frac{1}{\mathcal{Z}} \int \mathcal{D}[\psi]\,\mathcal{D}[\psi^*]\ \psi_\sigma(\tau_1)\psi^*_\sigma(\tau_2)\ \exp\Big[\mathcal{A}_0 - U\sum_{\sigma\sigma'}\int_0^\beta d\tau\,\psi^*_\sigma\psi_\sigma\psi^*_{\sigma'}\psi_{\sigma'}\Big]$$

- Discretization $\beta = \Lambda\,\Delta\tau$,
- Trotter decoupling $e^{-\beta(\hat{T}+\hat{V})} = \lim_{\Lambda\to\infty}\left[e^{-\Delta\tau\hat{T}}e^{-\Delta\tau\hat{V}}\right]^\Lambda$
- Discrete Hubbard-Stratonovich transformation $e^{\Delta\tau U(\hat{n}_\uparrow-\hat{n}_\downarrow)^2/2} = \frac{1}{2}\sum_{s=\pm1} e^{\lambda s(\hat{n}_\uparrow-\hat{n}_\downarrow)}$

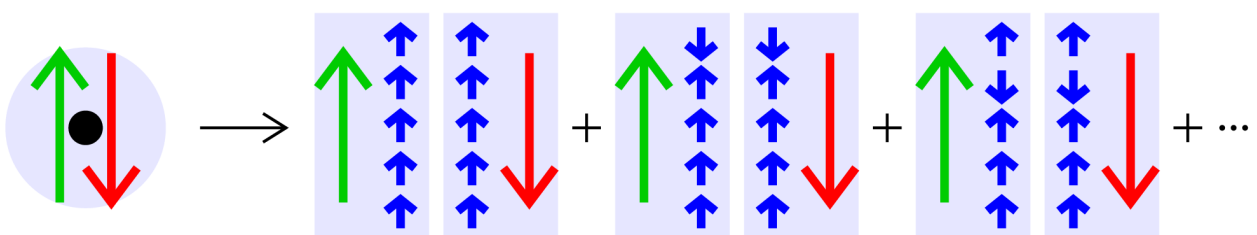

Wick theorem:

$$G = \frac{\sum M \det\{M\}}{\sum \det\{M\}}$$

Auxiliary-field QMC algorithm [Hirsch, Fye (1986)]

Green function G in imaginary time (fermionic Grassmann variables ψ, ψ^*):

$$G_\sigma(\tau_2-\tau_1) = \frac{1}{\mathcal{Z}} \int \mathcal{D}[\psi]\,\mathcal{D}[\psi^*]\ \psi_\sigma(\tau_1)\psi^*_\sigma(\tau_2)\ \exp\Big[\mathcal{A}_0 - U\sum_{\sigma\sigma'}\int_0^\beta d\tau\,\psi^*_\sigma\psi_\sigma\psi^*_{\sigma'}\psi_{\sigma'}\Big]$$

- Discretization $\beta = \Lambda\,\Delta\tau$,
- Trotter decoupling $e^{-\beta(\hat{T}+\hat{V})} = \lim_{\Lambda\to\infty}\left[e^{-\Delta\tau\hat{T}}e^{-\Delta\tau\hat{V}}\right]^\Lambda$
- Discrete Hubbard-Stratonovich transformation $e^{\Delta\tau U(\hat{n}_\uparrow-\hat{n}_\downarrow)^2/2} = \frac{1}{2}\sum_{s=\pm1} e^{\lambda s(\hat{n}_\uparrow-\hat{n}_\downarrow)}$

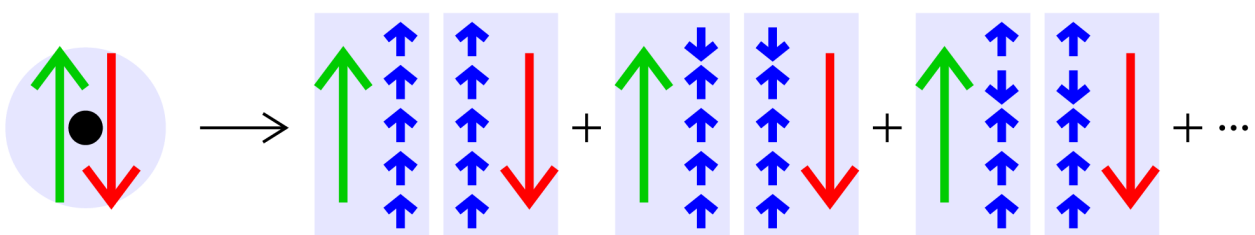

Wick theorem:

$$G = \frac{\sum M \det\{M\}}{\sum \det\{M\}}$$

Metropolis MC importance sampling over auxiliary Ising field $\{s\}$: 2^Λ configurations

\+ numerically exact, + no sign problem, − effort scales as T^{-3}

Special issue: Fourier transformations in DMFT-QMC cycle

Iterative solution of DMFT equations (for imaginary-time impurity solver)

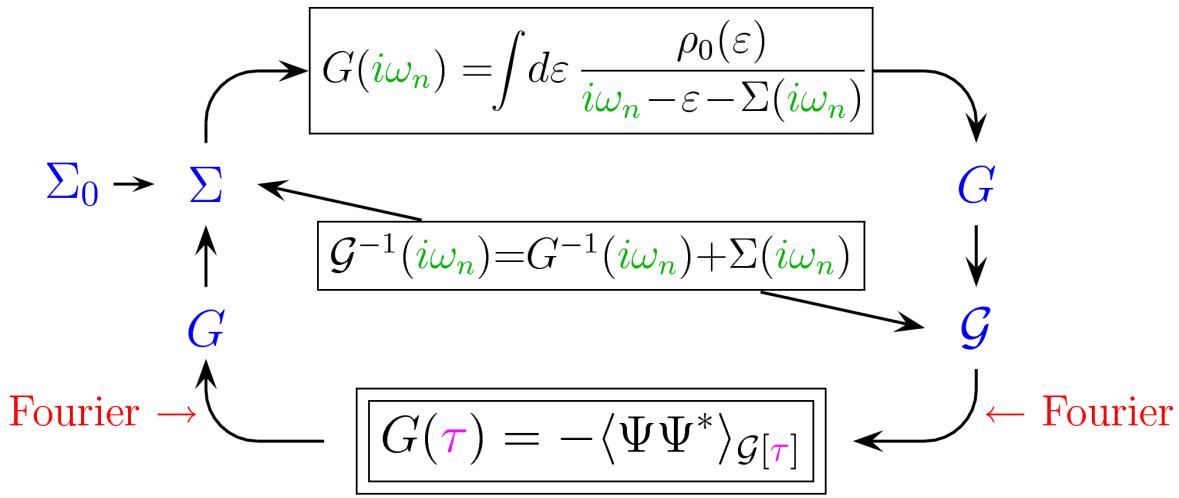

Special issue: Fourier transformations in DMFT-QMC cycle

Iterative solution of DMFT equations (for imaginary-time impurity solver)

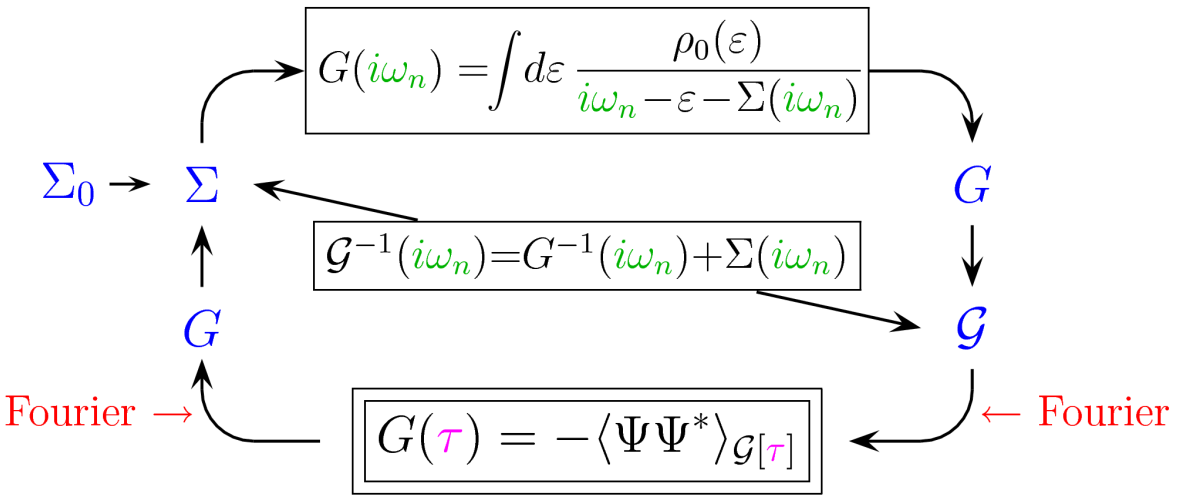

Naive discrete Fourier transformation $\rightsquigarrow$ oscillations (instead of $G(\omega) \overset{\omega\to\infty}{\longrightarrow} 1/\omega$)

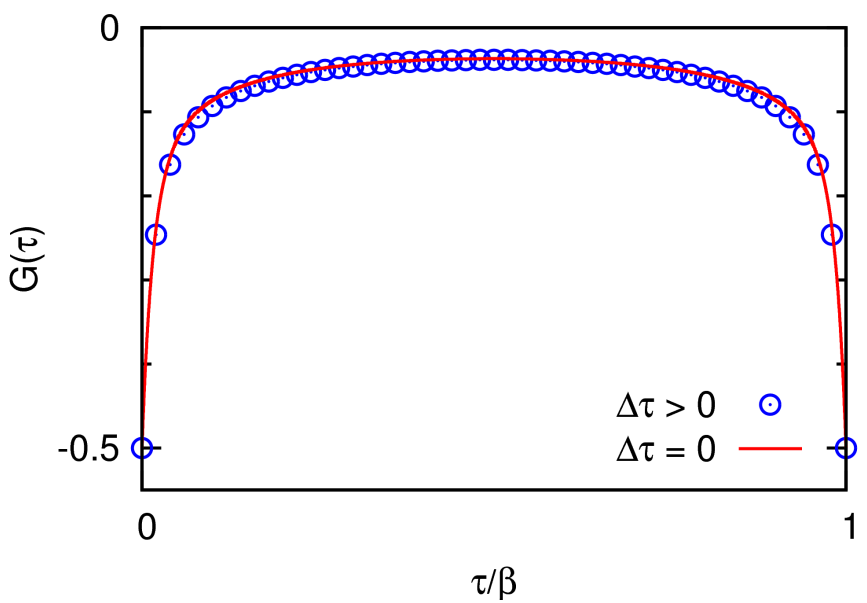

naive FT $\longrightarrow$

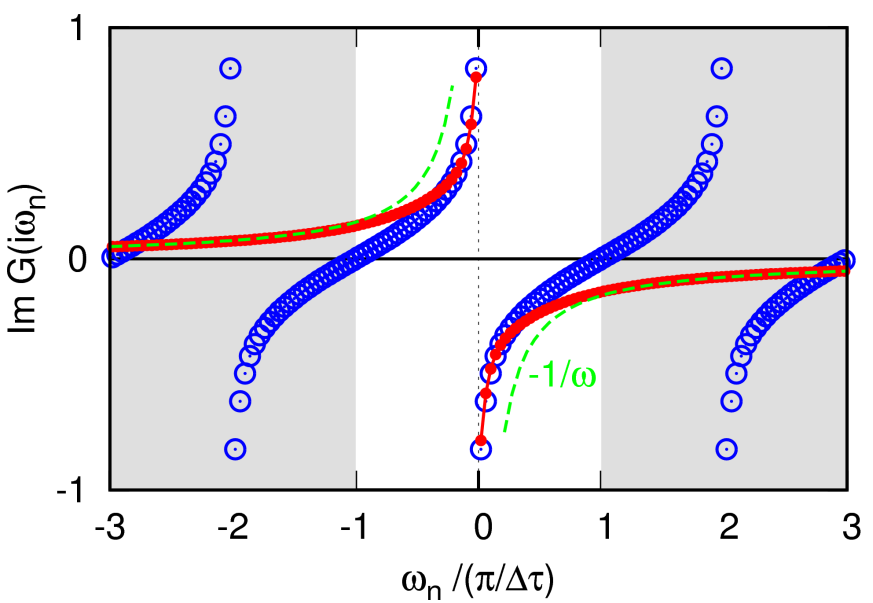

Best solution: interpolate $G_{\mathrm{QMC}}(\tau)$, e.g., by cubic splines [Jarrell, Krauth, Gull, . . .]

But: $\dfrac{d^2G(\tau)}{d\tau^2}$ maximal for $\tau \to 0, \beta$ $\rightsquigarrow$ natural boundary conditions inappropriate

Best solution: interpolate $G_{\mathrm{QMC}}(\tau)$, e.g., by cubic splines [Jarrell, Krauth, Gull, . . .]

But: $\dfrac{d^2G(\tau)}{d\tau^2}$ maximal for $\tau \to 0, \beta$ $\rightsquigarrow$ natural boundary conditions inappropriate

- adjust boundary cond. [Oudovenko]
- spline-fit only difference w.r.t. reference problem:
  - IPT [Jarrell]

Best solution: interpolate $G_{\mathrm{QMC}}(\tau)$, e.g., by cubic splines [Jarrell, Krauth, Gull, . . .]

But: $\dfrac{d^2G(\tau)}{d\tau^2}$ maximal for $\tau \to 0, \beta$ $\rightsquigarrow$ natural boundary conditions inappropriate

- adjust boundary cond. [Oudovenko]
- spline-fit only difference w.r.t. reference problem:
  - IPT [Jarrell]
  - high-frequency expansion for $\Sigma(\omega)$ + param. [Knecht, NB]

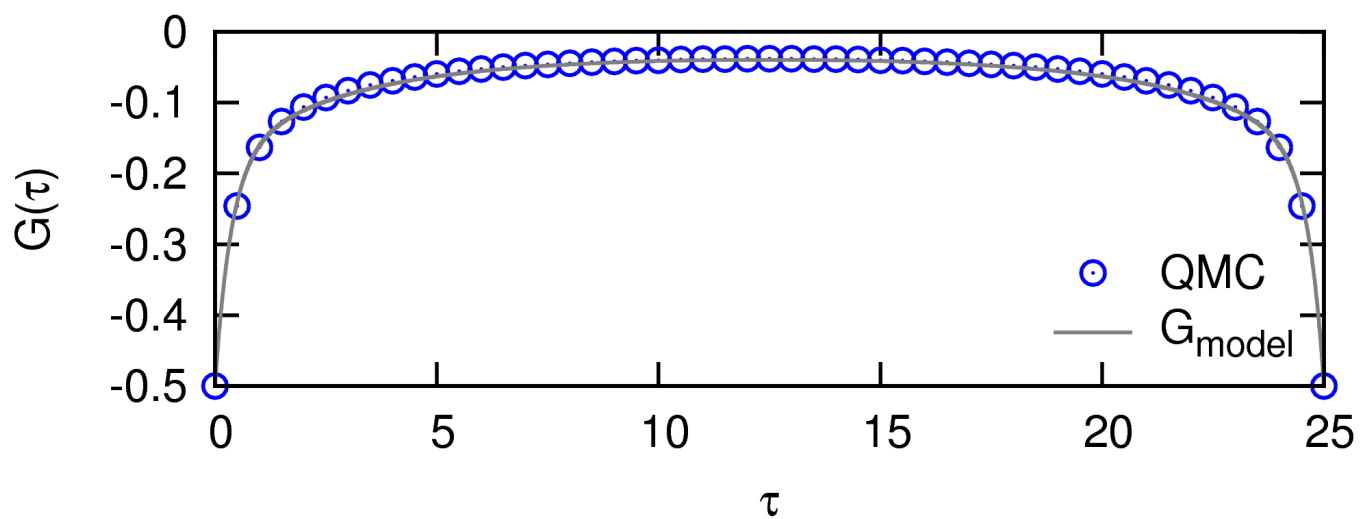

$$\Sigma_\sigma(\omega) = U\left(\langle\hat{n}_{-\sigma}\rangle - \tfrac{1}{2}\right)\omega^0 + U^2\langle\hat{n}_{-\sigma}\rangle\left(1 - \langle\hat{n}_{-\sigma}\rangle\right)\omega^{-1} + \mathcal{O}(\omega^{-2})$$

Best solution: interpolate $G_{\mathrm{QMC}}(\tau)$, e.g., by cubic splines [Jarrell, Krauth, Gull, . . .]

But: $\dfrac{d^2G(\tau)}{d\tau^2}$ maximal for $\tau \to 0, \beta$ $\rightsquigarrow$ natural boundary conditions inappropriate

- adjust boundary cond. [Oudovenko]
- spline-fit only difference w.r.t. reference problem:
  - IPT [Jarrell]
  - high-frequency expansion for $\Sigma(\omega)$ + param. [Knecht, NB]

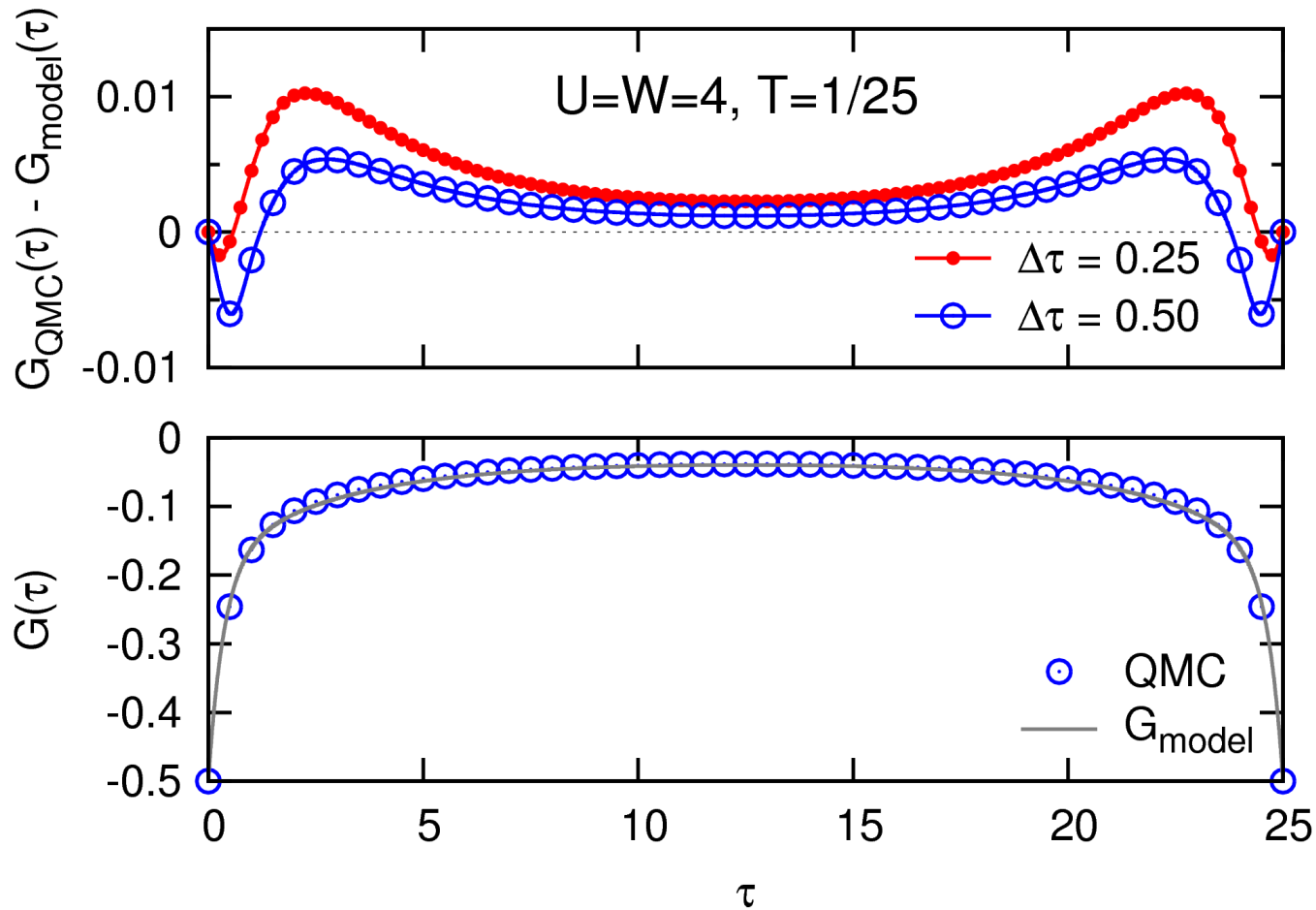

$$\Sigma_\sigma(\omega) = U\left(\langle \hat{n}_{-\sigma}\rangle - \tfrac{1}{2}\right)\omega^0 + U^2\langle \hat{n}_{-\sigma}\rangle\left(1 - \langle \hat{n}_{-\sigma}\rangle\right)\omega^{-1} + \mathcal{O}(\omega^{-2})$$

Mott transition within DMFT

Fully frustrated 1-band model,
energy scale: bandwidth $W = 4$

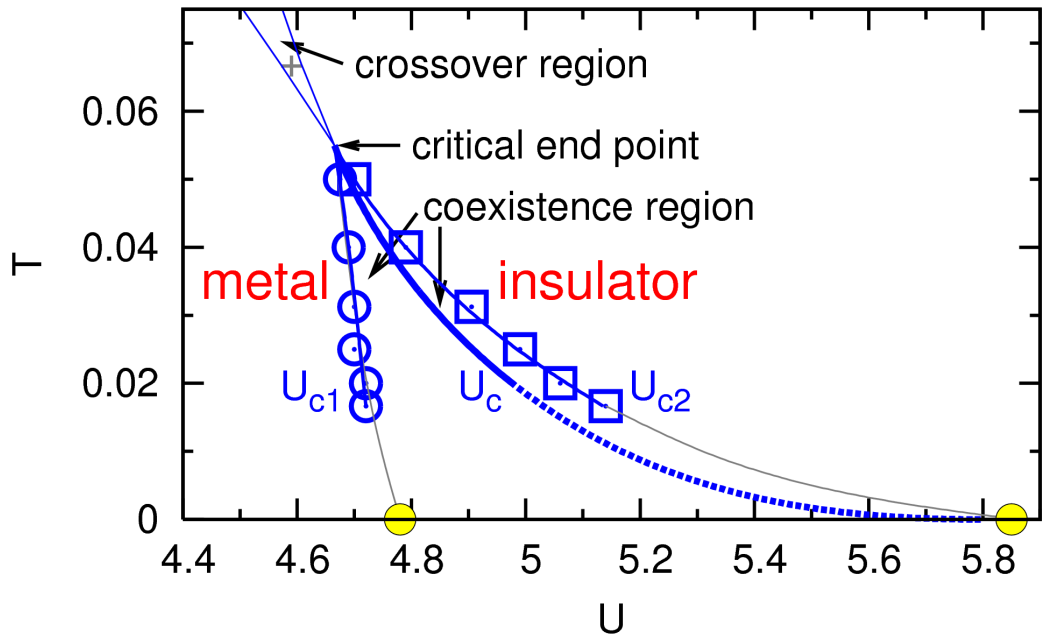

Mott transition within DMFT

Fully frustrated 1-band model,
energy scale: bandwidth $W = 4$

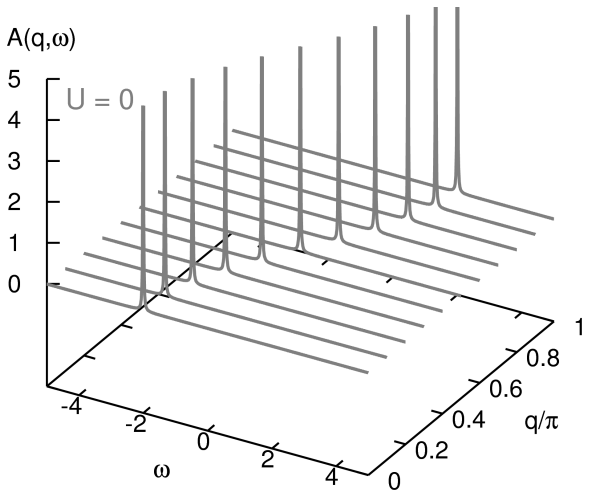

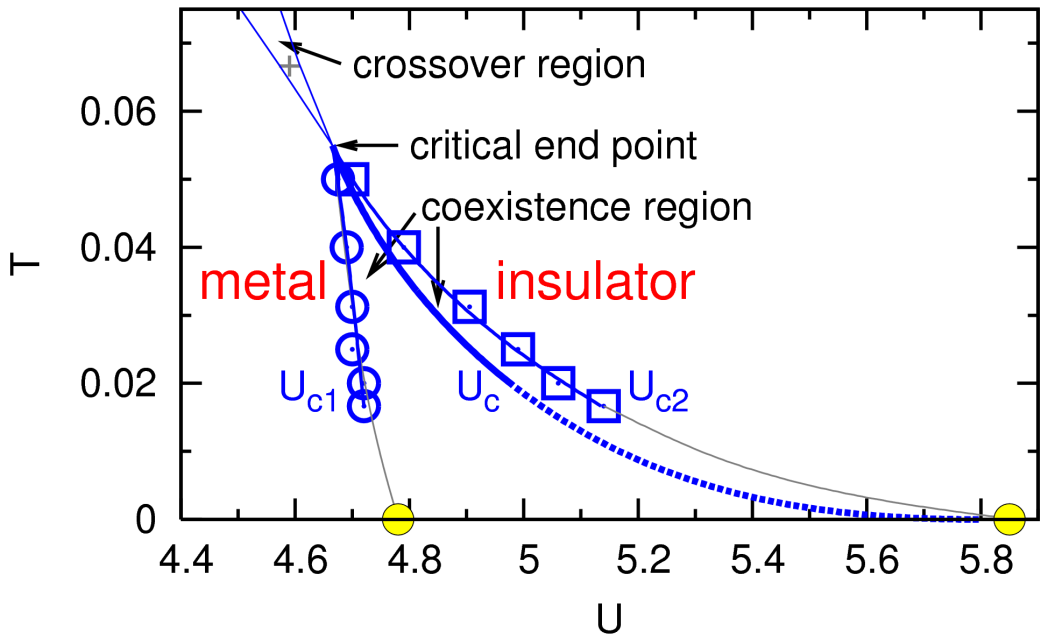

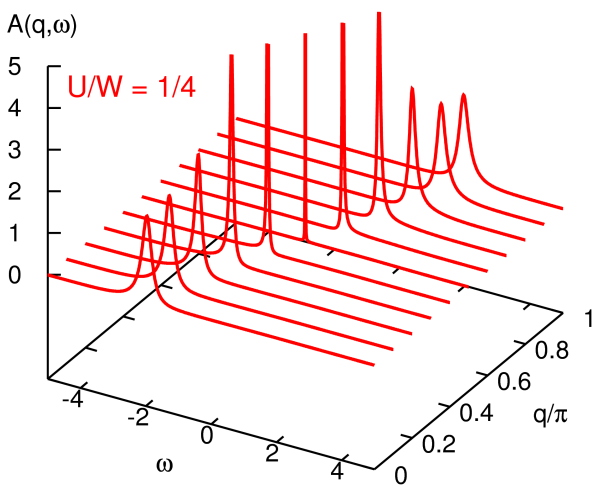

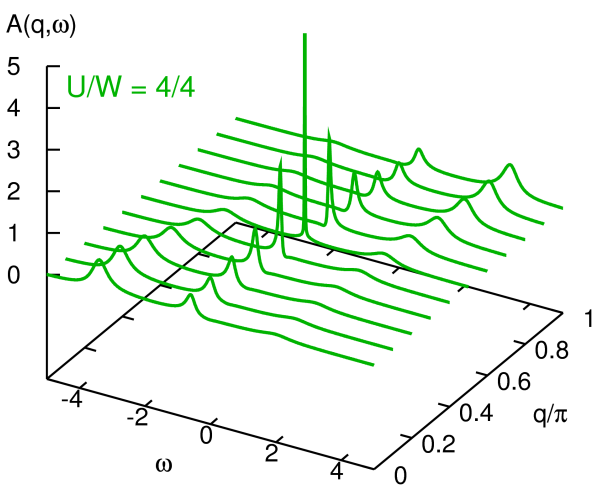

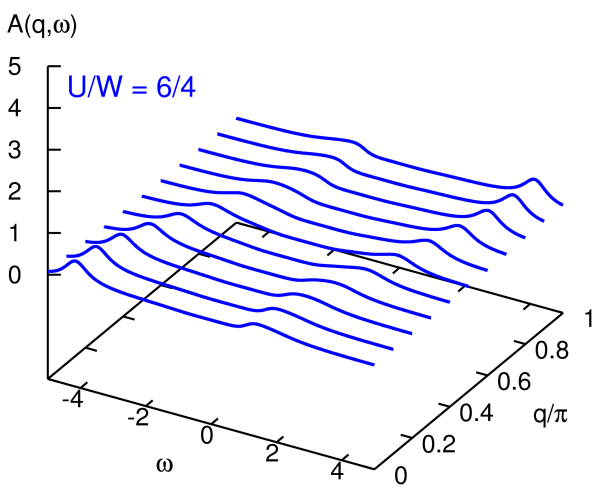

Efficiency of QMC DMFT solvers

New development: continuous-time QMC algorithms

1. weak-coupling expansion

[Rubtsov, Savkin, Lichtenstein, PRB (2005)]

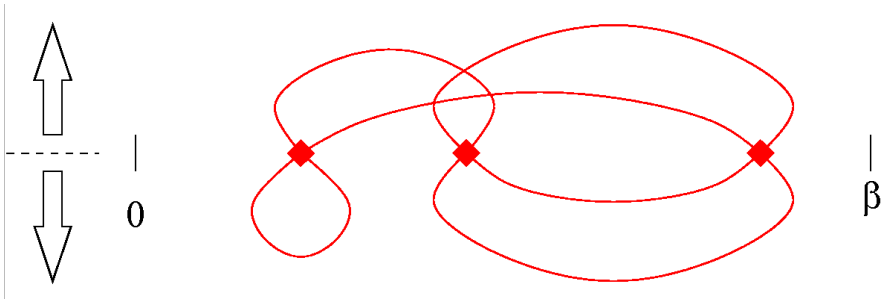

2. hybridization expansion

[Werner et al., PRL (2006)]

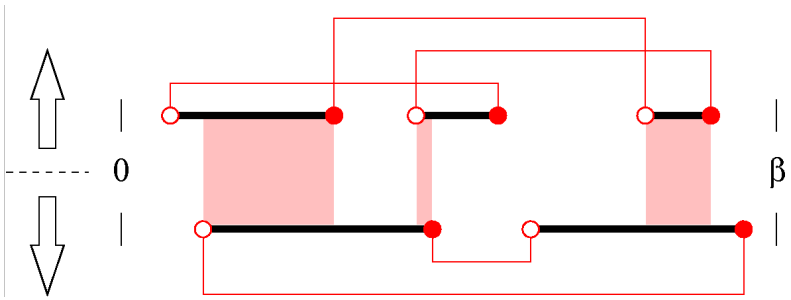

Efficiency of QMC DMFT solvers

New development: continuous-time QMC algorithms

1. weak-coupling expansion

[Rubtsov, Savkin, Lichtenstein, PRB (2005)]

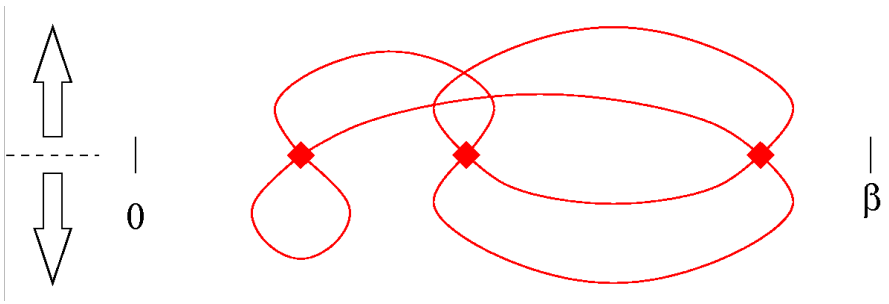

2. hybridization expansion

[Werner et al., PRL (2006)]

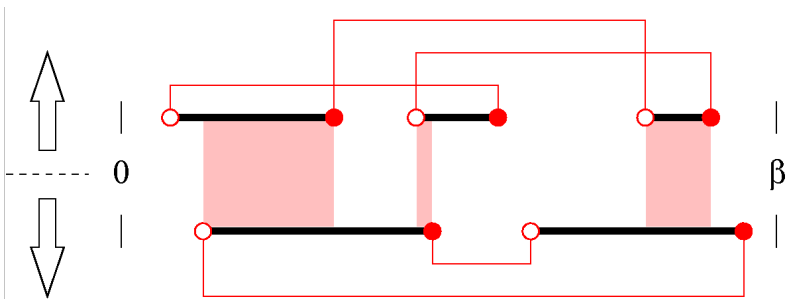

CT-QMC methods: smaller matrices

All QMC methods: effort $\propto \Lambda^3$

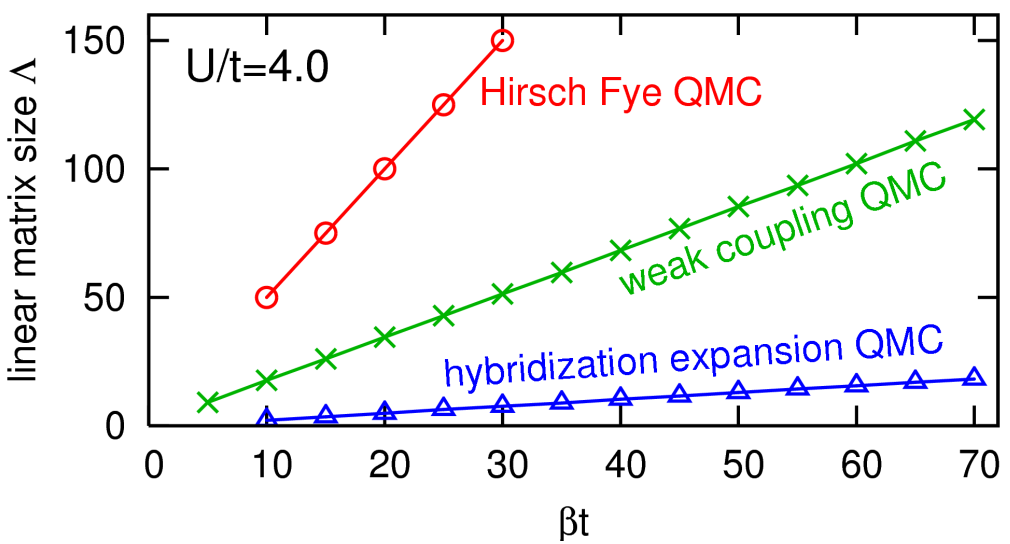

Efficiency of QMC DMFT solvers

New development: continuous-time QMC algorithms

1. weak-coupling expansion

[Rubtsov, Savkin, Lichtenstein, PRB (2005)]

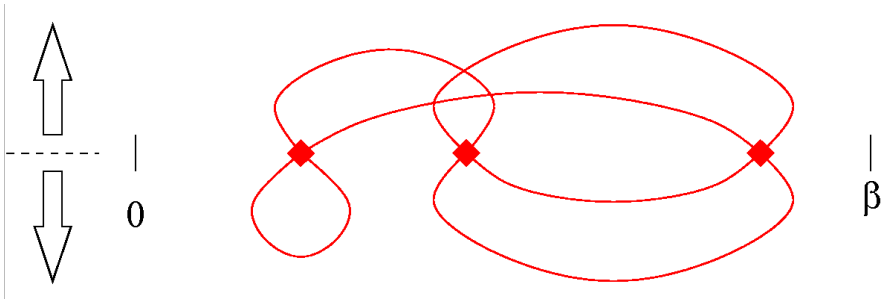

2. hybridization expansion

[Werner et al., PRL (2006)]

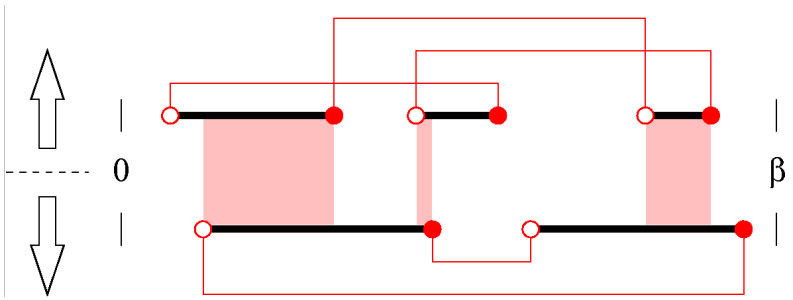

CT-QMC methods: smaller matrices

All QMC methods: effort $\propto \Lambda^3$

Claim [Troyer (2006)]:
"CT-QMC more efficient than HF-QMC by orders of magnitude"

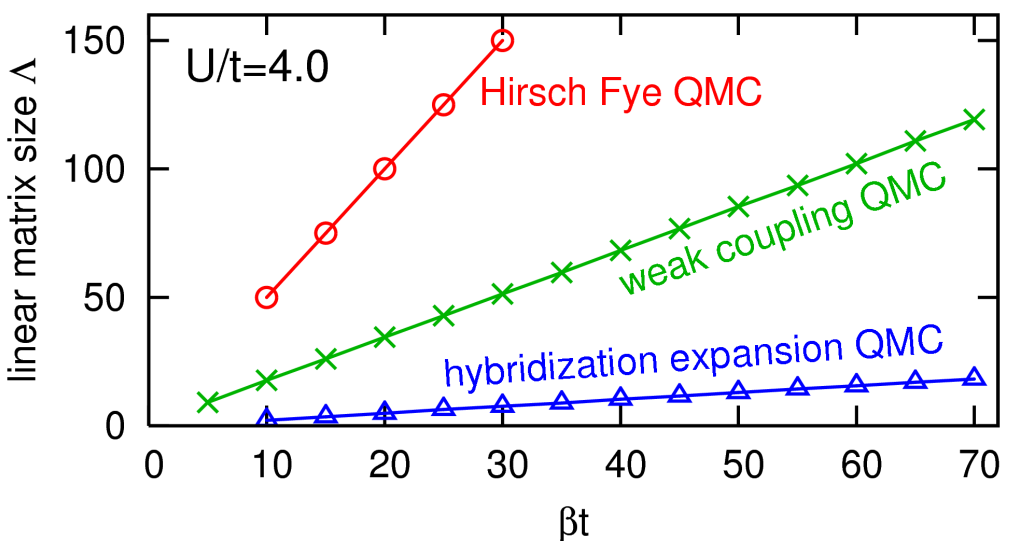

Comparison of QMC DMFT solvers: self energy (at $U = W = 4$)

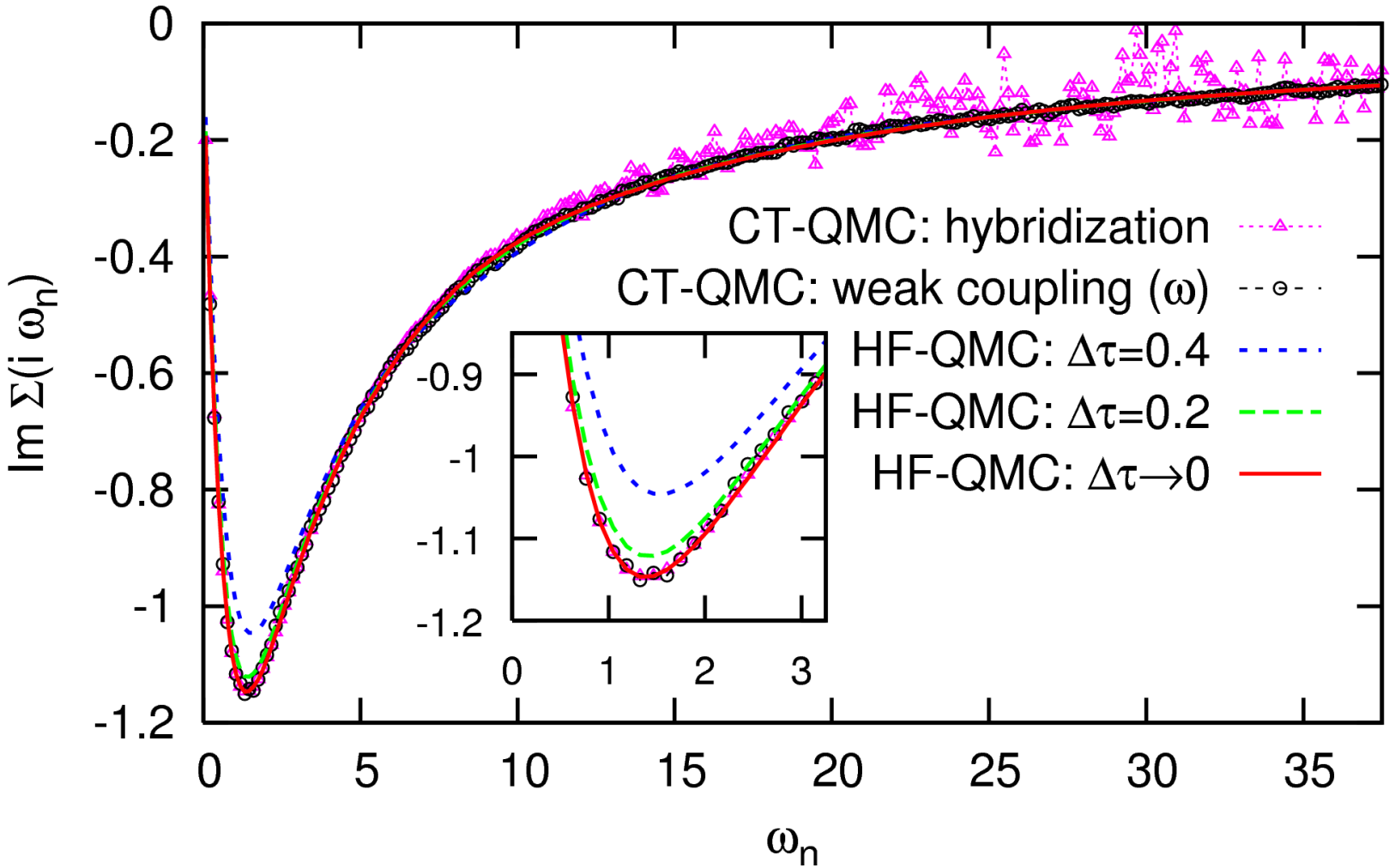

hybridization CT-QMC: strong fluctuations at large frequencies

HF-QMC: systematic errors only at small frequencies [NB, PRB **76**, 205120 (2007)]

Comparisons at constant CPU time: kinetic energy (at $U = W = 4$)

140 CPU hours on AMD Opteron 244 (serial) / mix of Opterons (parallel)

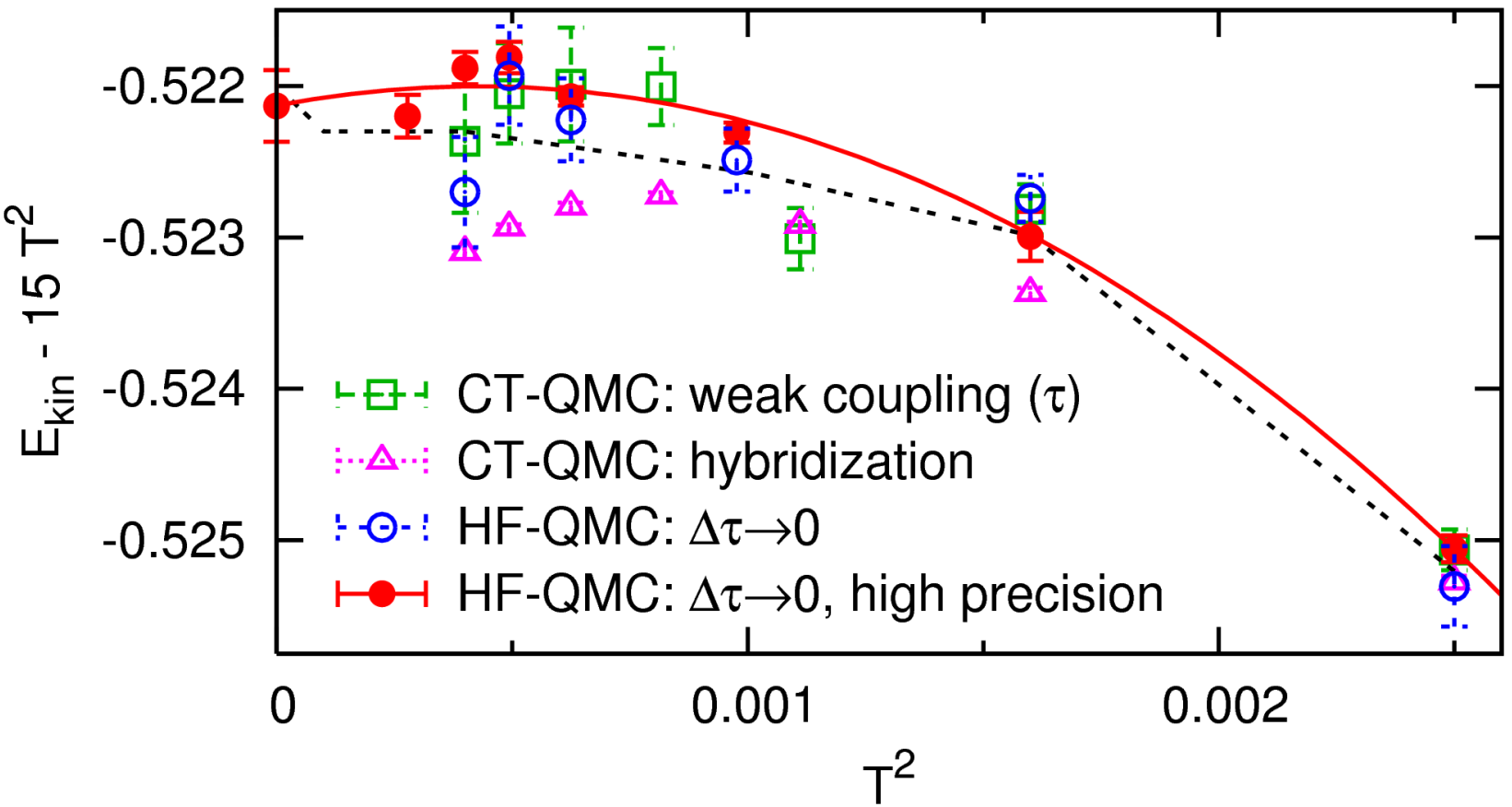

Similar precision for HF-QMC and weak-coupling CT-QMC

Systematic errors in hybridization CT-QMC data! [NB, PRB **76**, 205120 (2007)]

Comparison for total energy (at $U = W = 4$)

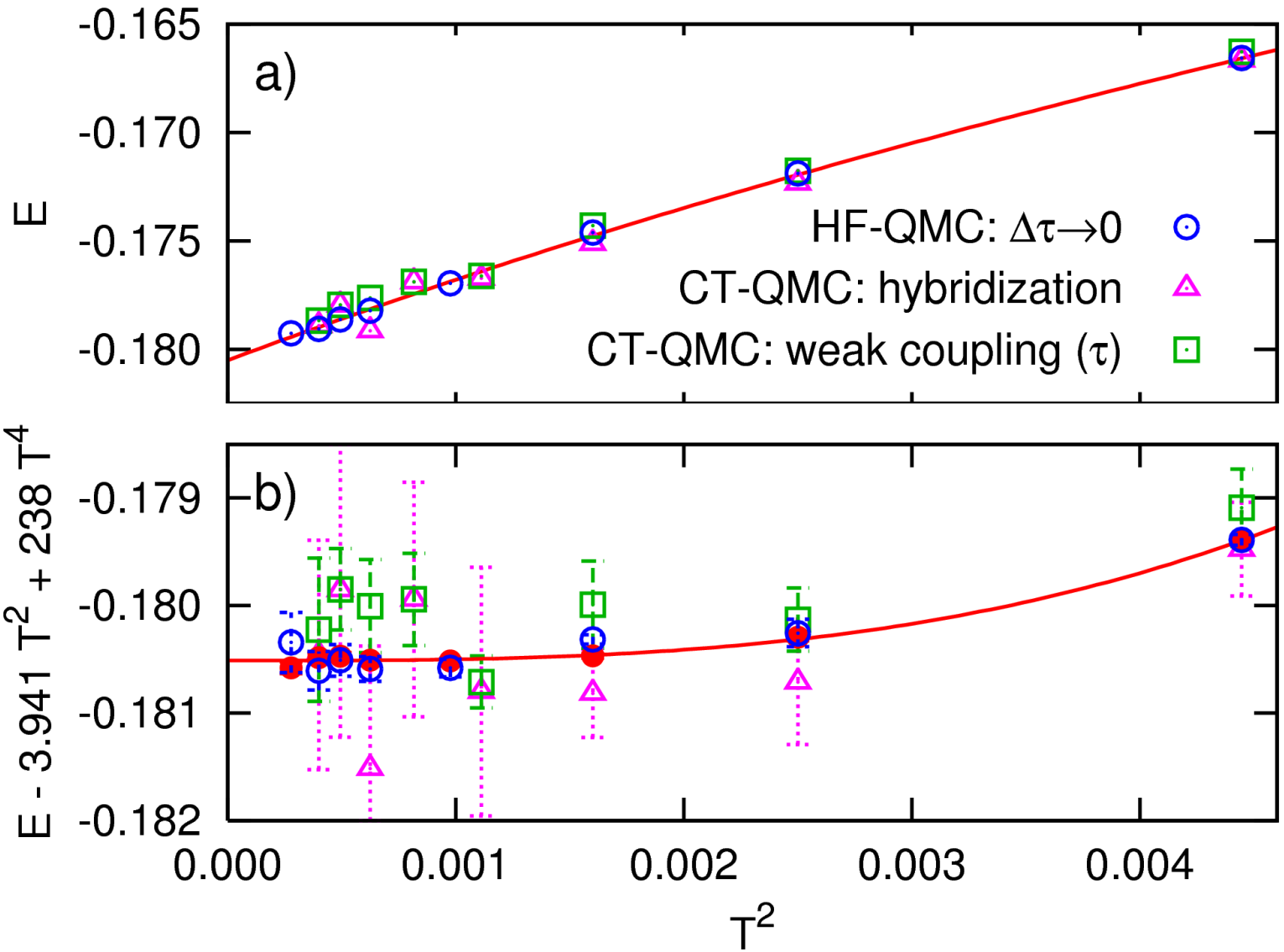

HF-QMC more efficient (higher precision at same cost) [NB, PRB **76**, 205120 (2007)]

Unbiased Green functions and spectra from HF-QMC

State of the art: analytic continuation (using MEM) of imaginary-time Green function at fixed finite (often large) $\Delta\tau$ $\rightsquigarrow$ bias

Unbiased Green functions and spectra from HF-QMC

State of the art: analytic continuation (using MEM) of imaginary-time Green function at fixed finite (often large) $\Delta\tau$ $\rightsquigarrow$ bias

Reason: no obvious extrapolation scheme for $G(\tau)$

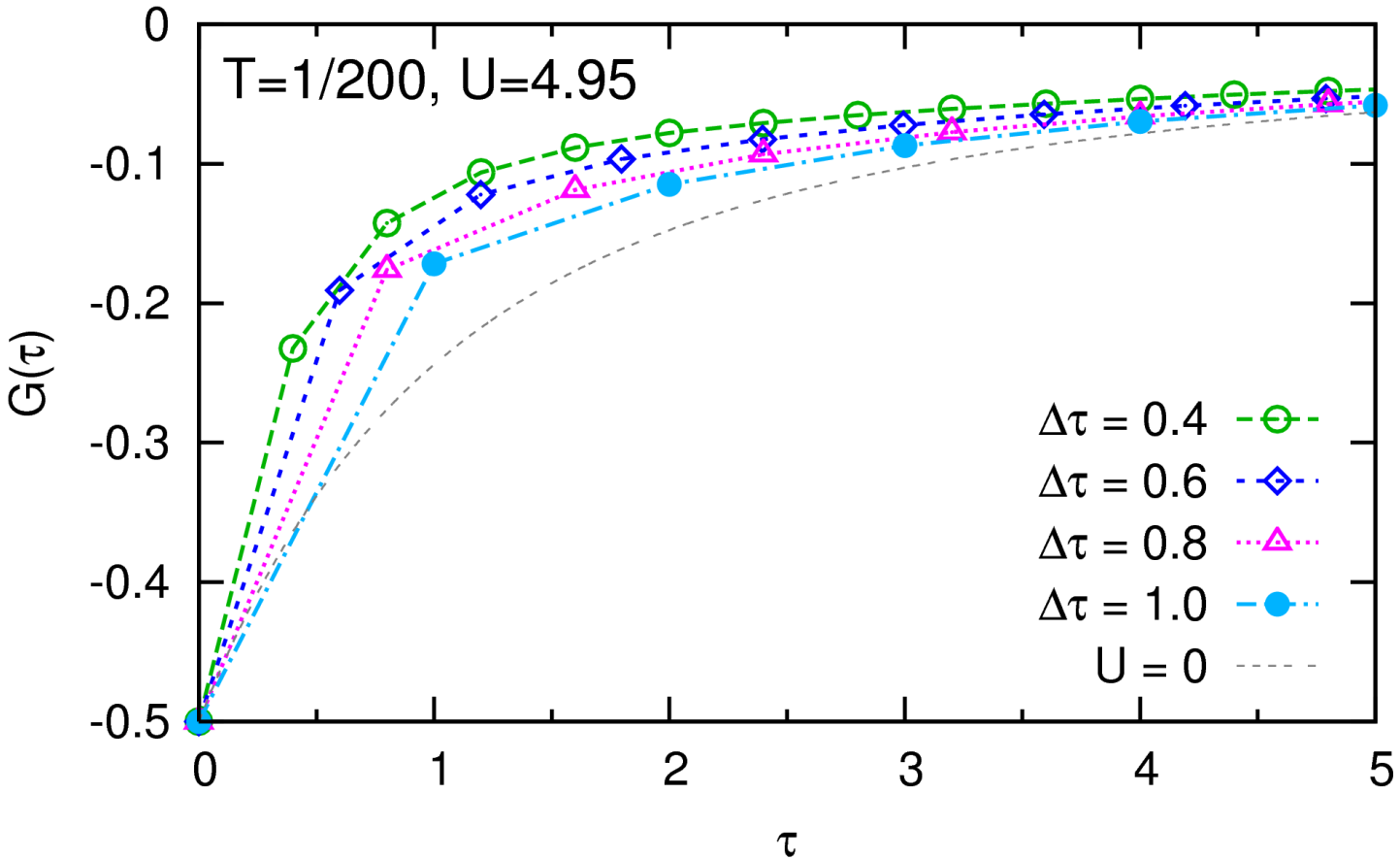

Low temperature ("beyond HF-QMC"): large $\Delta\tau$ $\rightsquigarrow$ large biases [NB, arXiv:0712.1290]

Unbiased Green functions and spectra from HF-QMC

State of the art: analytic continuation (using MEM) of imaginary-time Green function at fixed

Reason: no obvious extrapolatic

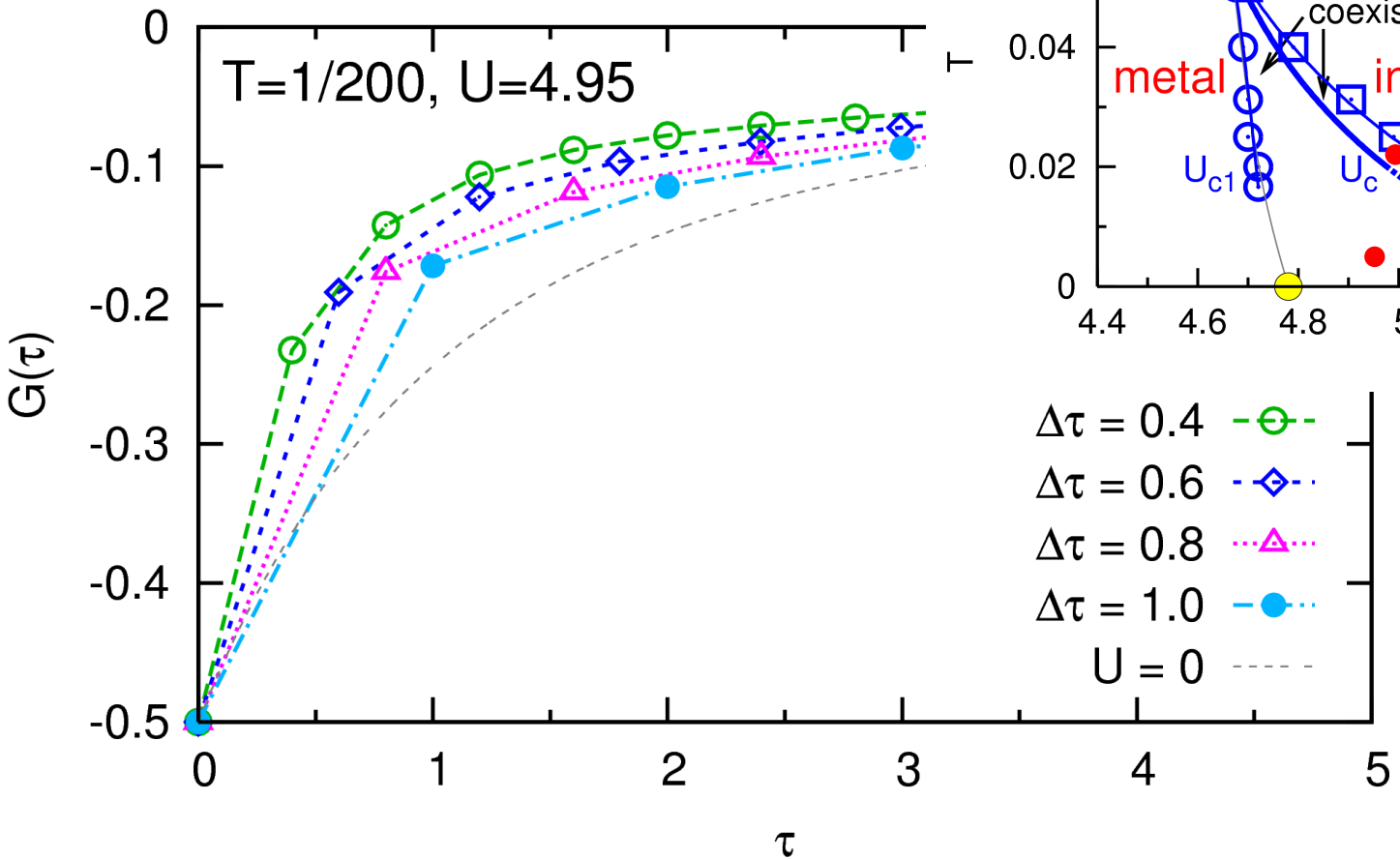

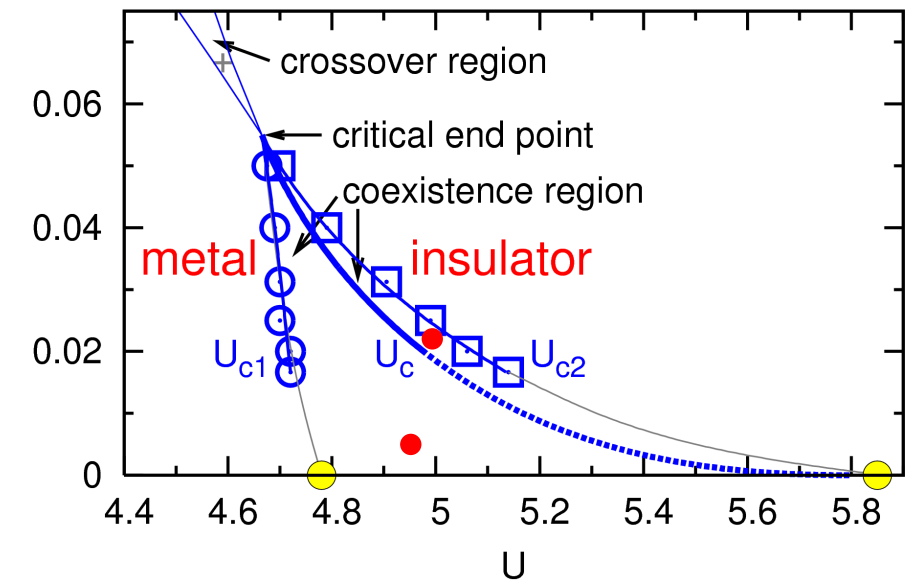

Low temperature ("beyond HF-QMC"): large $\Delta\tau \rightsquigarrow$ large biases [NB, arXiv:0712.1290]

Unbiased Green functions and spectra from HF-QMC

State of the art: analytic continuation (using MEM) of imaginary-time Green function at fixed finite (often large) $\Delta\tau$ $\rightsquigarrow$ bias

Reason: no obvious extrapolation scheme for $G(\tau)$

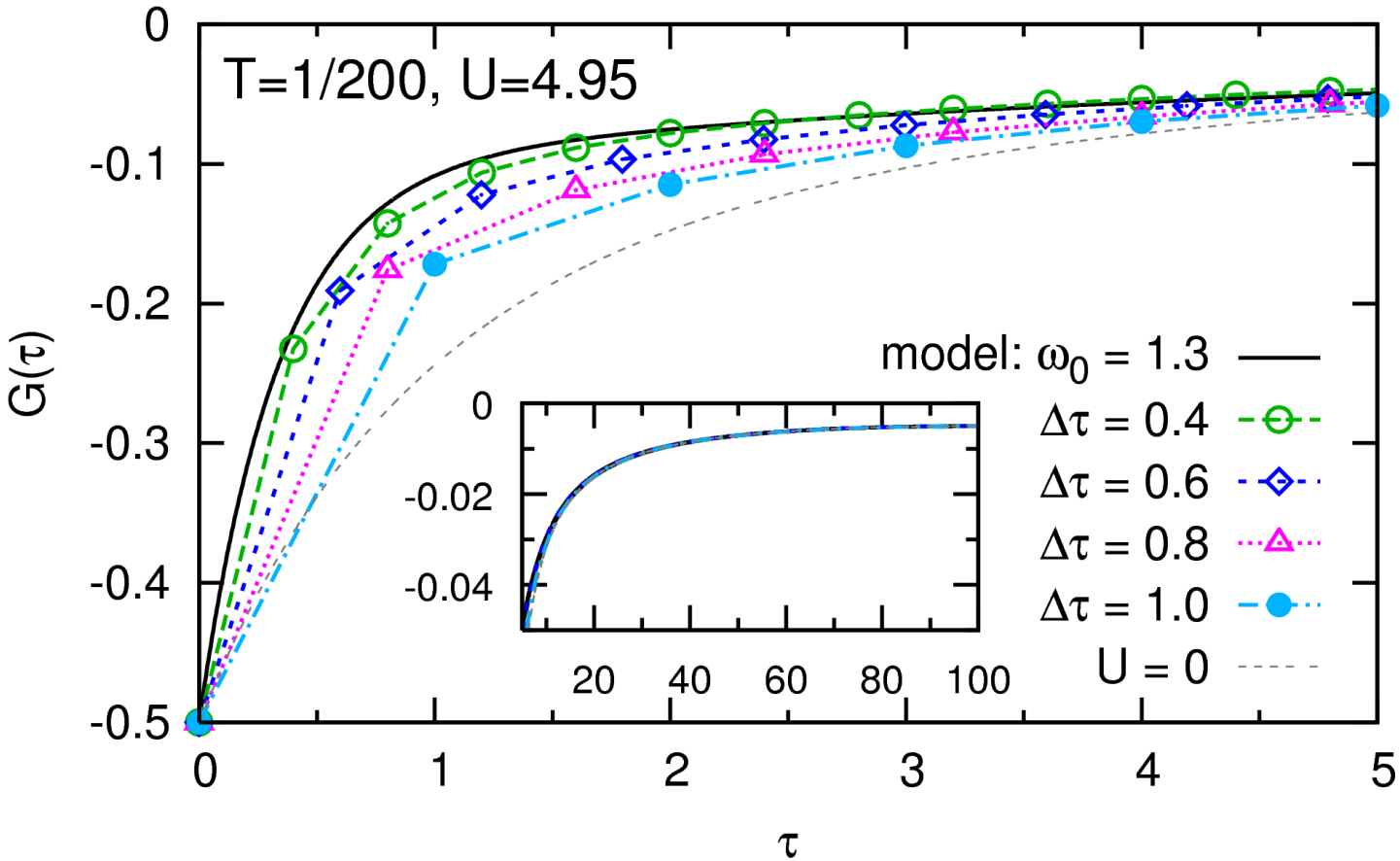

Low temperature ("beyond HF-QMC"): large $\Delta\tau$ $\rightsquigarrow$ large biases [NB, arXiv:0712.1290]

New Green function extrapolation scheme

For each $\Delta\tau$:
- average $G_{\Delta\tau}(\tau)$ over parallel runs for same impurity model
- average $\log[-G_{\Delta\tau}(\tau)]$ over iterations ($\sim$ geometric av. for $G_{\Delta\tau}(\tau)$)
- interpolate via difference Green function $G_{\Delta\tau}(\tau) - G_{\text{model}}(\tau)$

$\rightsquigarrow$ $G_{\Delta\tau_1}$, $G_{\Delta\tau_2}$, . . . $G_{\Delta\tau_n}$ (with error bars) on common fine τ grid

New Green function extrapolation scheme

For each $\Delta\tau$:
- average $G_{\Delta\tau}(\tau)$ over parallel runs for same impurity model
- average $\log[-G_{\Delta\tau}(\tau)]$ over iterations ($\sim$ geometric av. for $G_{\Delta\tau}(\tau)$)
- interpolate via difference Green function $G_{\Delta\tau}(\tau) - G_{\text{model}}(\tau)$

$\rightsquigarrow$ $G_{\Delta\tau_1}$, $G_{\Delta\tau_2}$, ... $G_{\Delta\tau_n}$ (with error bars) on common fine τ grid

- Extrapolate $\log[-G(\tau)]$ using cubic least-squares fits, overweighting low $\Delta\tau$

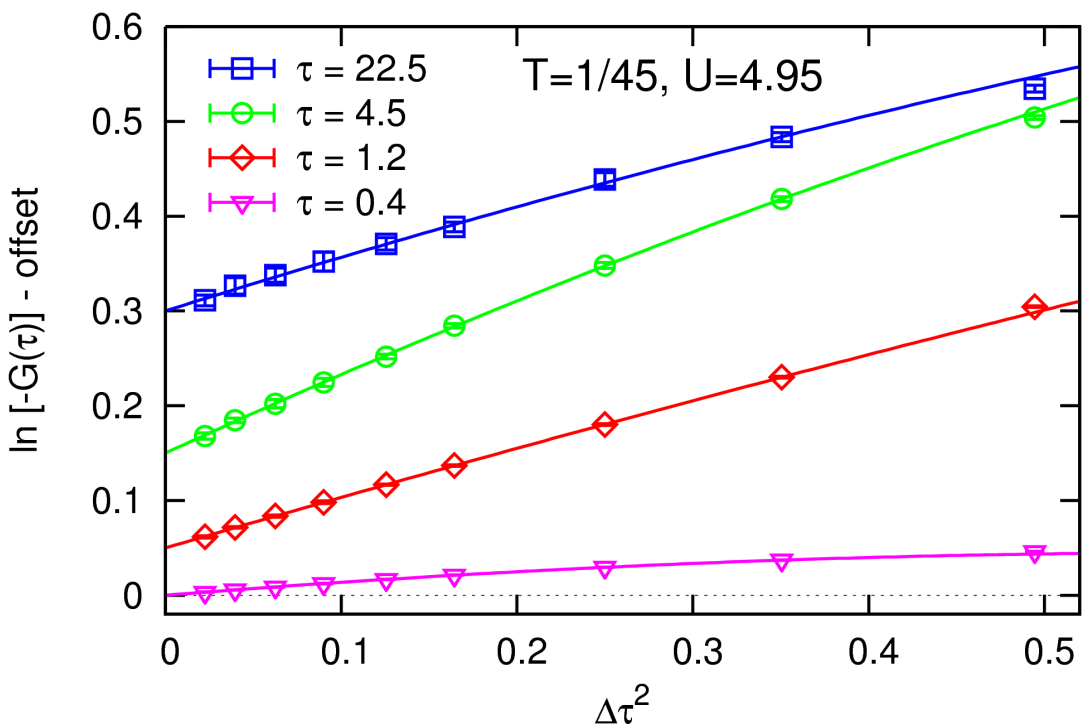

Result: unbiased, numerically exact Green function

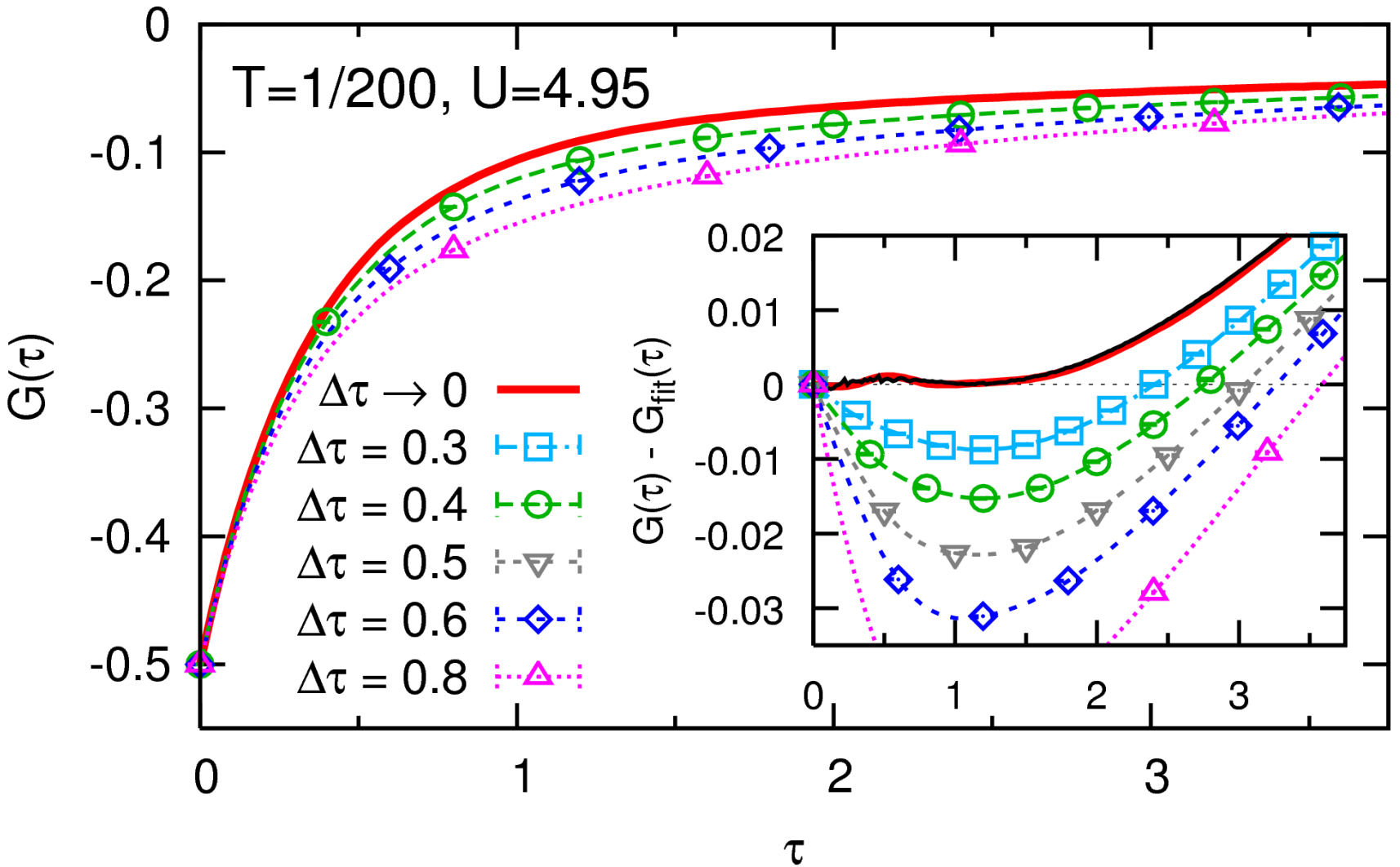

[NB, arXiv:0712.1290]

Excellent agreement with hybridization expansion CT-QMC [Werner et al., PRL (2006)]

2nd and 1st order derivatives of Green function

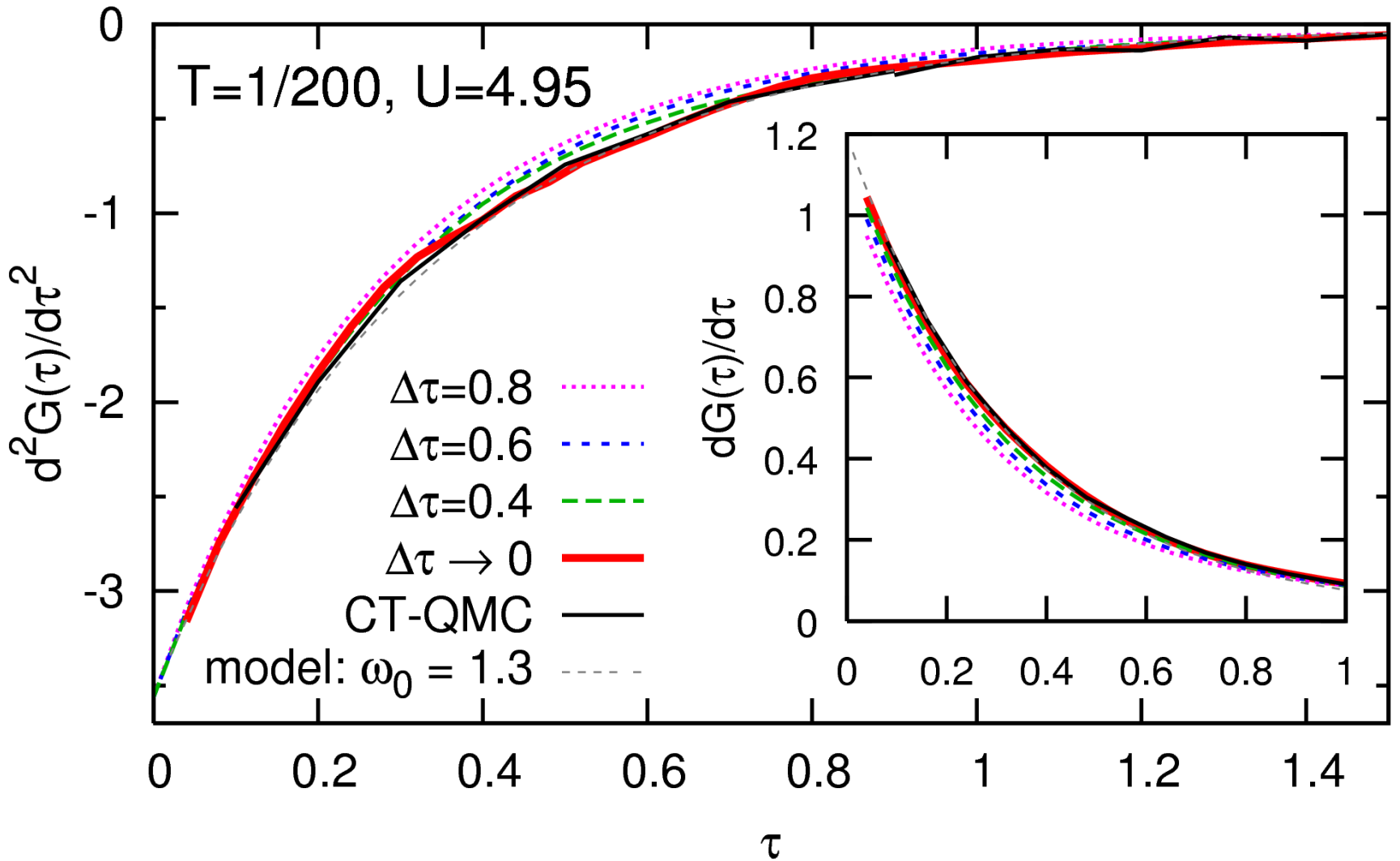

Exact asymptotics $\left.\frac{d^2G(\tau)}{d\tau^2}\right|_{\tau=0+} = \frac{1}{2} + \frac{U^2}{8}$; $\left.\frac{dG(\tau)}{d\tau}\right|_{\tau=0+}$ nonuniversal

Why average and extrapolation on logarithmic scale?

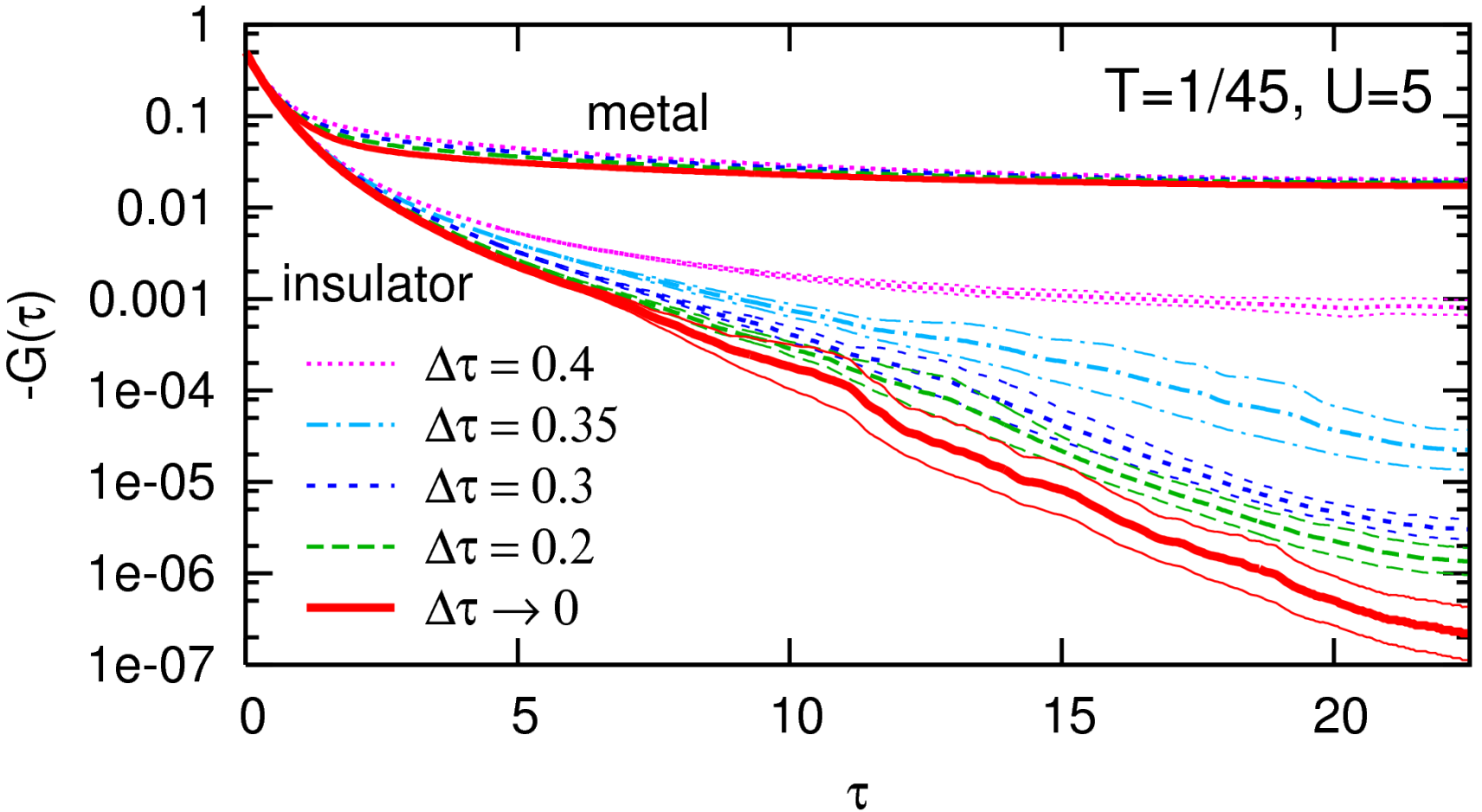

Difference metal–insulator and $\Delta\tau$ dependence involve orders of magnitude!

Even maximum statistical/iteration errors nearly order of magnitude

Low-τ resolution limited by $\Delta\tau$? No!

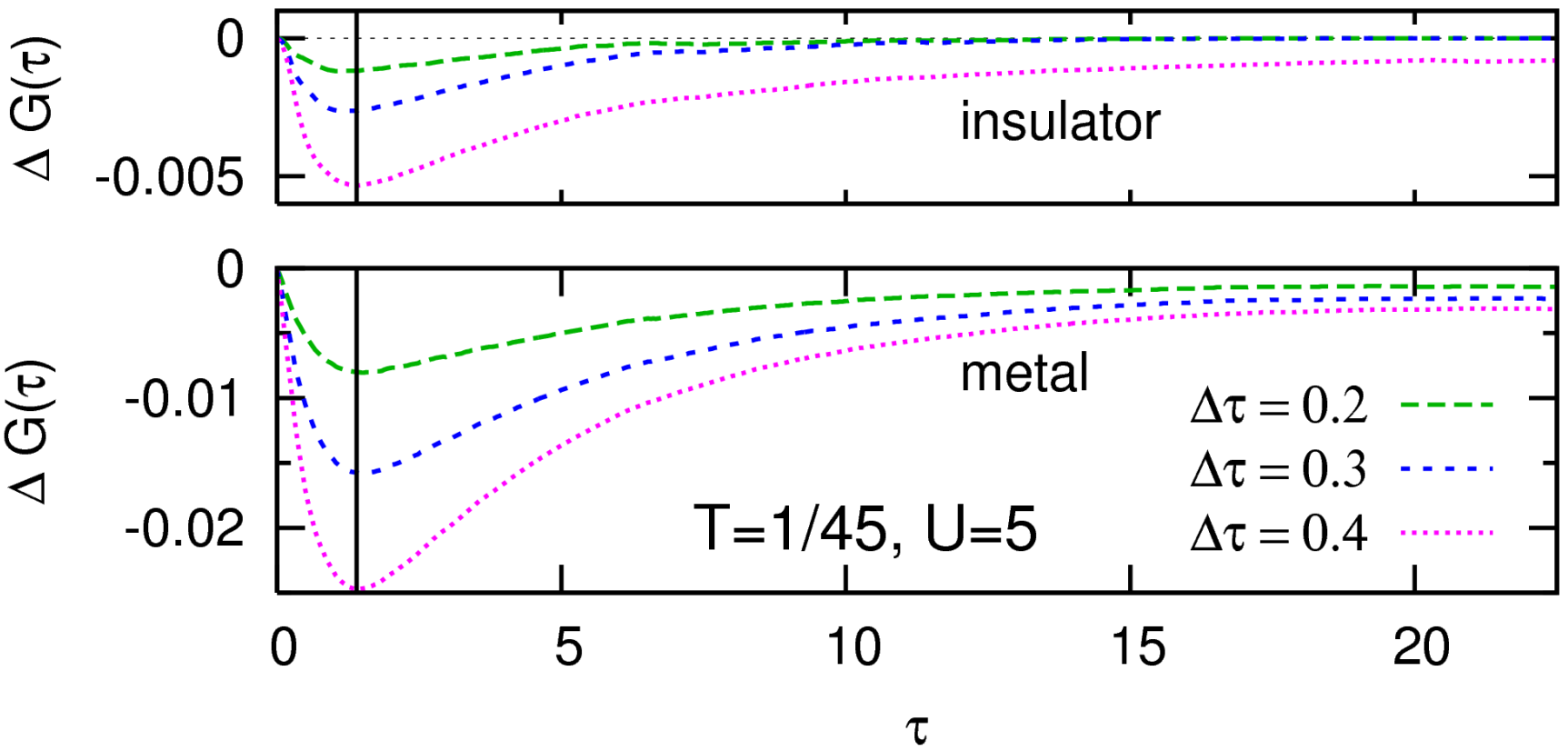

Uniform $\Delta\tau$ dependence, position of max. error independent of $\Delta\tau$ and phase!

Analytic continuation using Padé approximant for self-energy

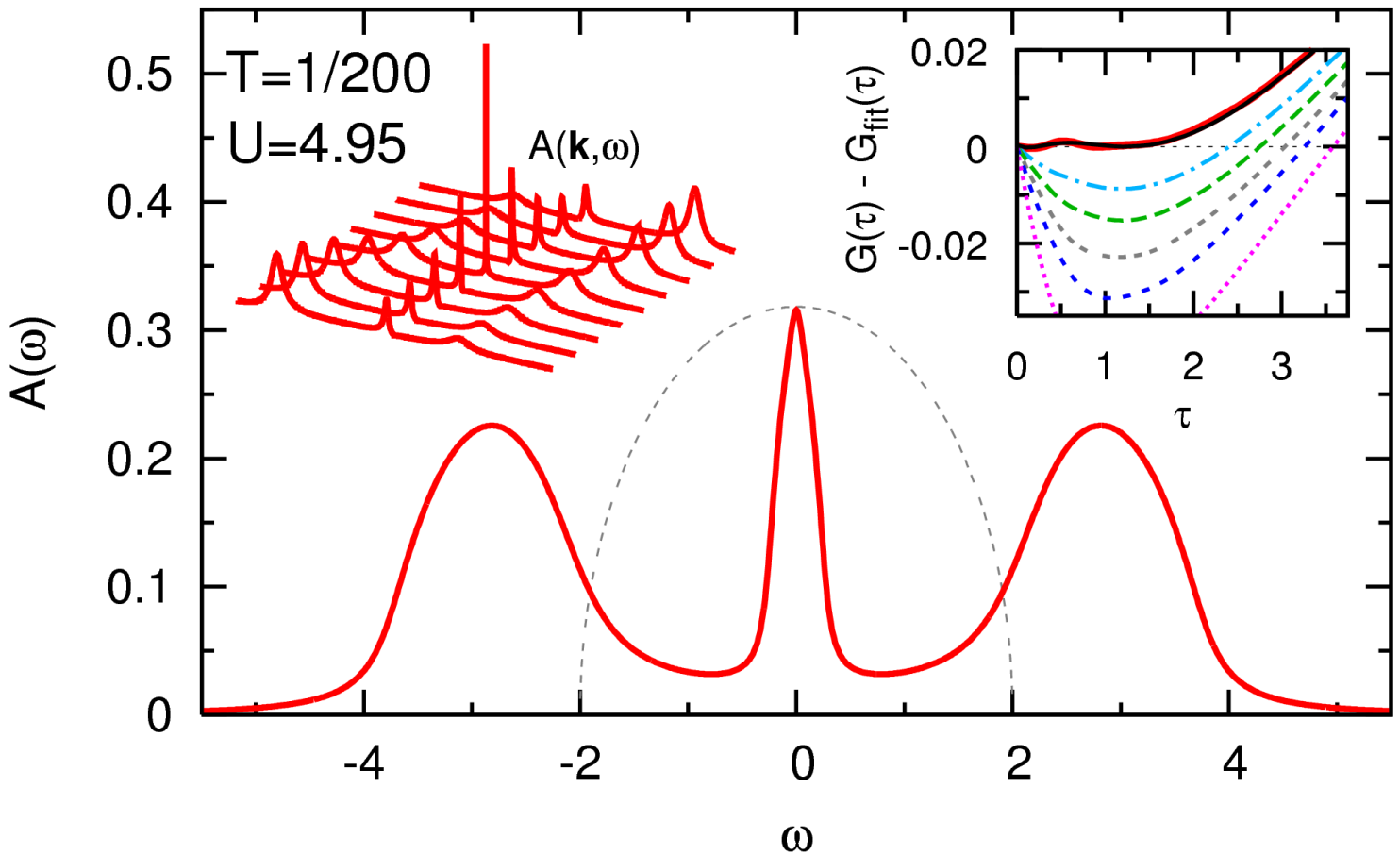

First spectra without discretization error from HF-QMC, at ultra-low T

Method directly applicable, e.g., to LDA+DMFT calculations [NB, arXiv:0712.1290]

Multigrid Hirsch-Fye quantum Monte Carlo algorithm

State of the art: (a) conventional HF-QMC

(b) *a posteriori* extrapolation of selected observables

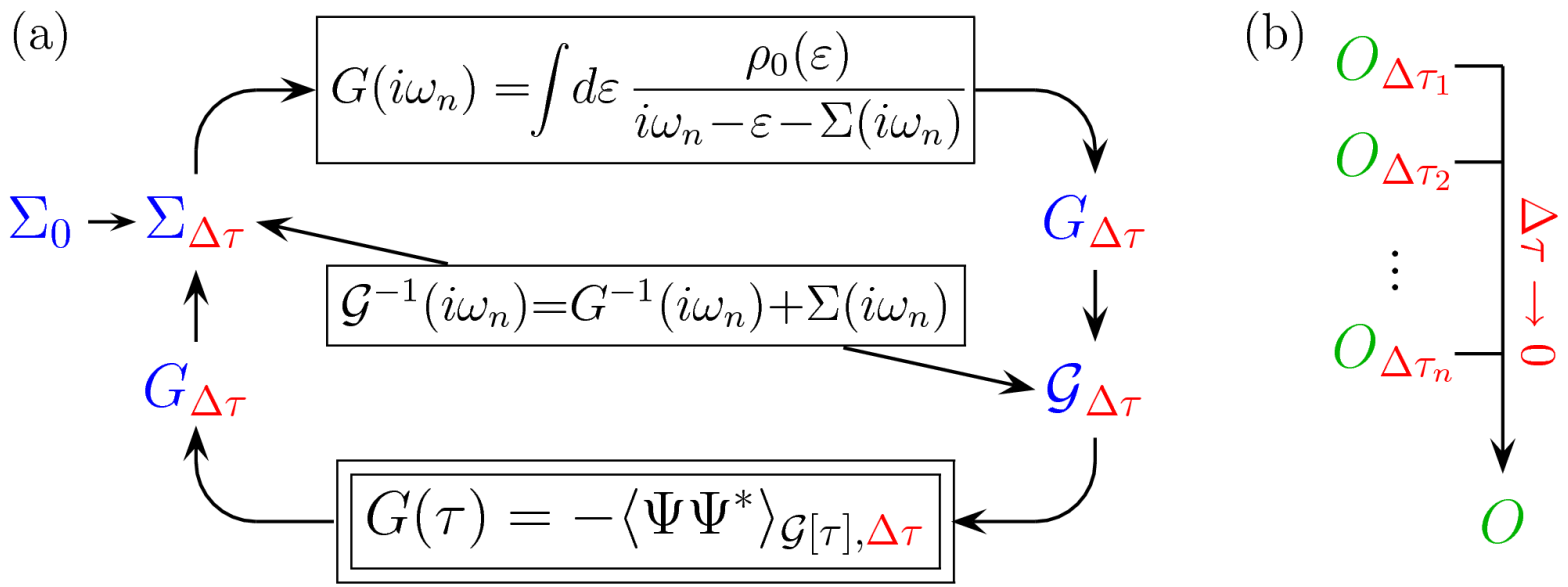

Multigrid Hirsch-Fye quantum Monte Carlo algorithm

State of the art: (a) conventional HF-QMC

(b) *a posteriori* extrapolation of selected observables

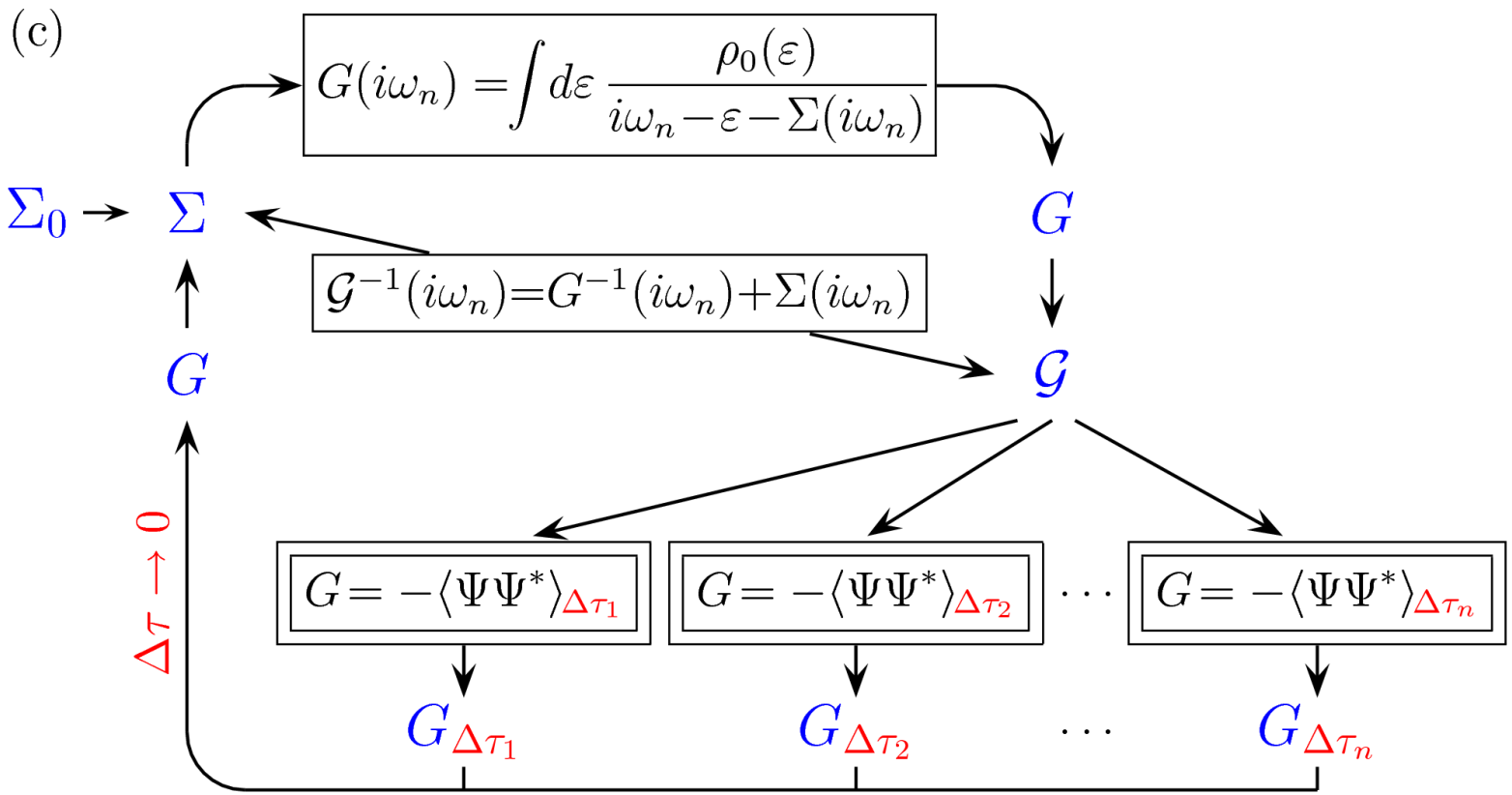

(c) Multigrid HF-QMC: internal elimination of Trotter error

$\rightsquigarrow$ quasi continuous time algorithm [NB, arXiv:0801.1222]

Schematic comparison via generalized Ginzburg-Landau functionals

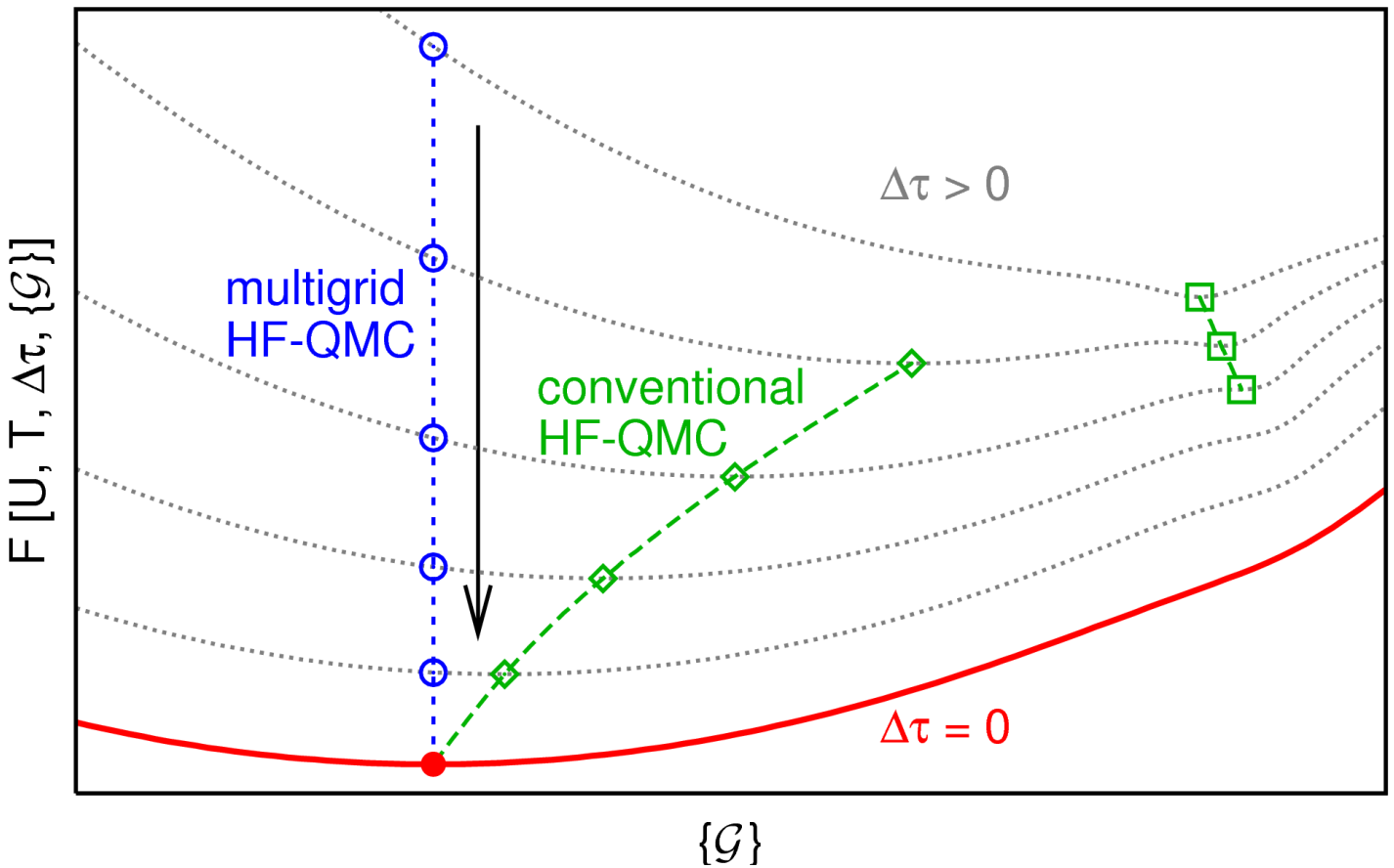

Conventional Hirsch-Fye QMC: DMFT fixed point shifts with $\Delta\tau$

Multigrid Hirsch-Fye QMC: DMFT iteration towards exact fixed point

Schematic comparison via generalized Ginzburg-Landau functionals

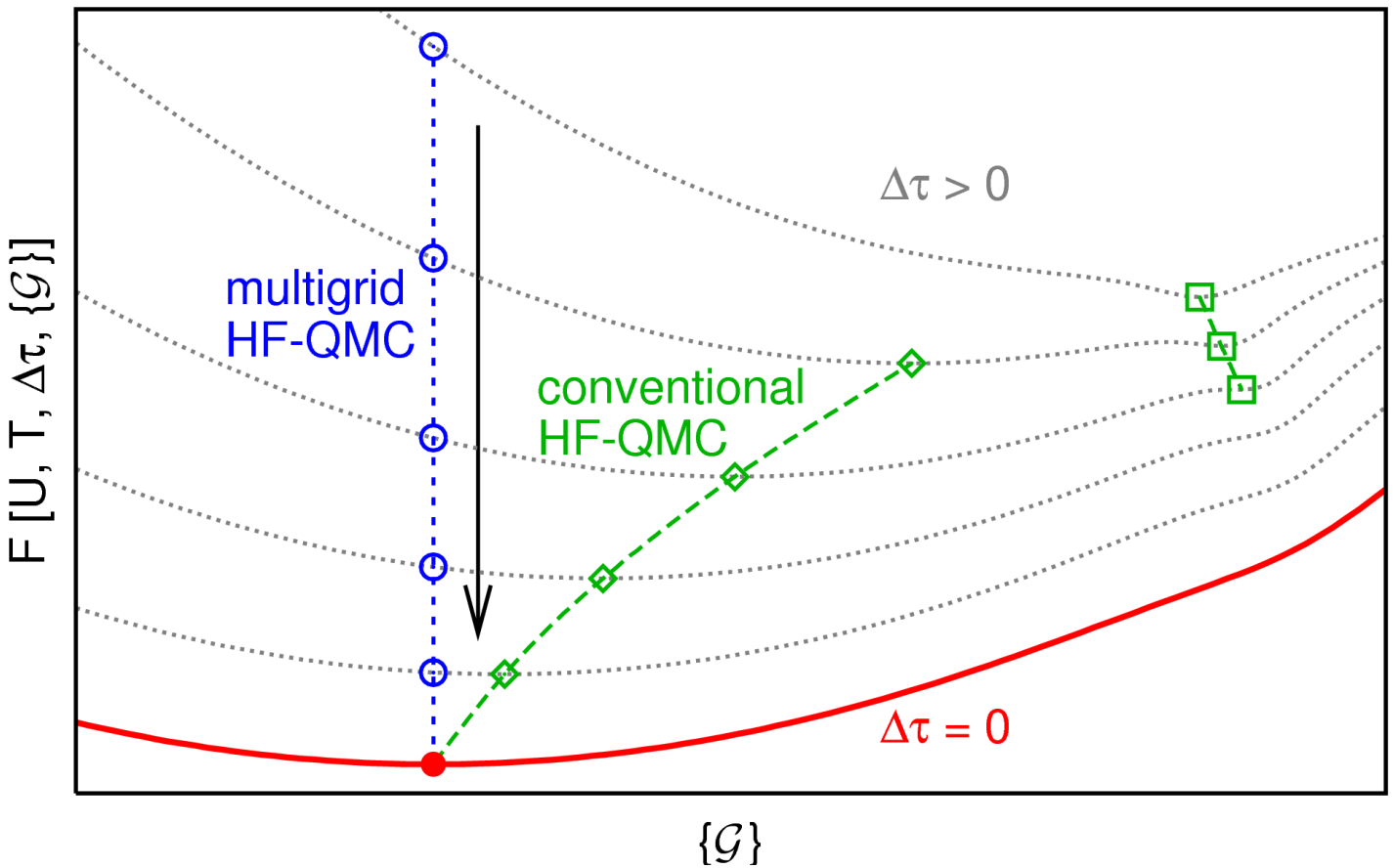

Conventional Hirsch-Fye QMC: DMFT fixed point shifts with $\Delta\tau$

Multigrid Hirsch-Fye QMC: DMFT iteration towards exact fixed point

Implementation: Green function extrapolation, hierarchy of frequency scales

Comparison: double occupancy $D = \langle n_{i\uparrow} n_{i\downarrow} \rangle$ near Mott transition

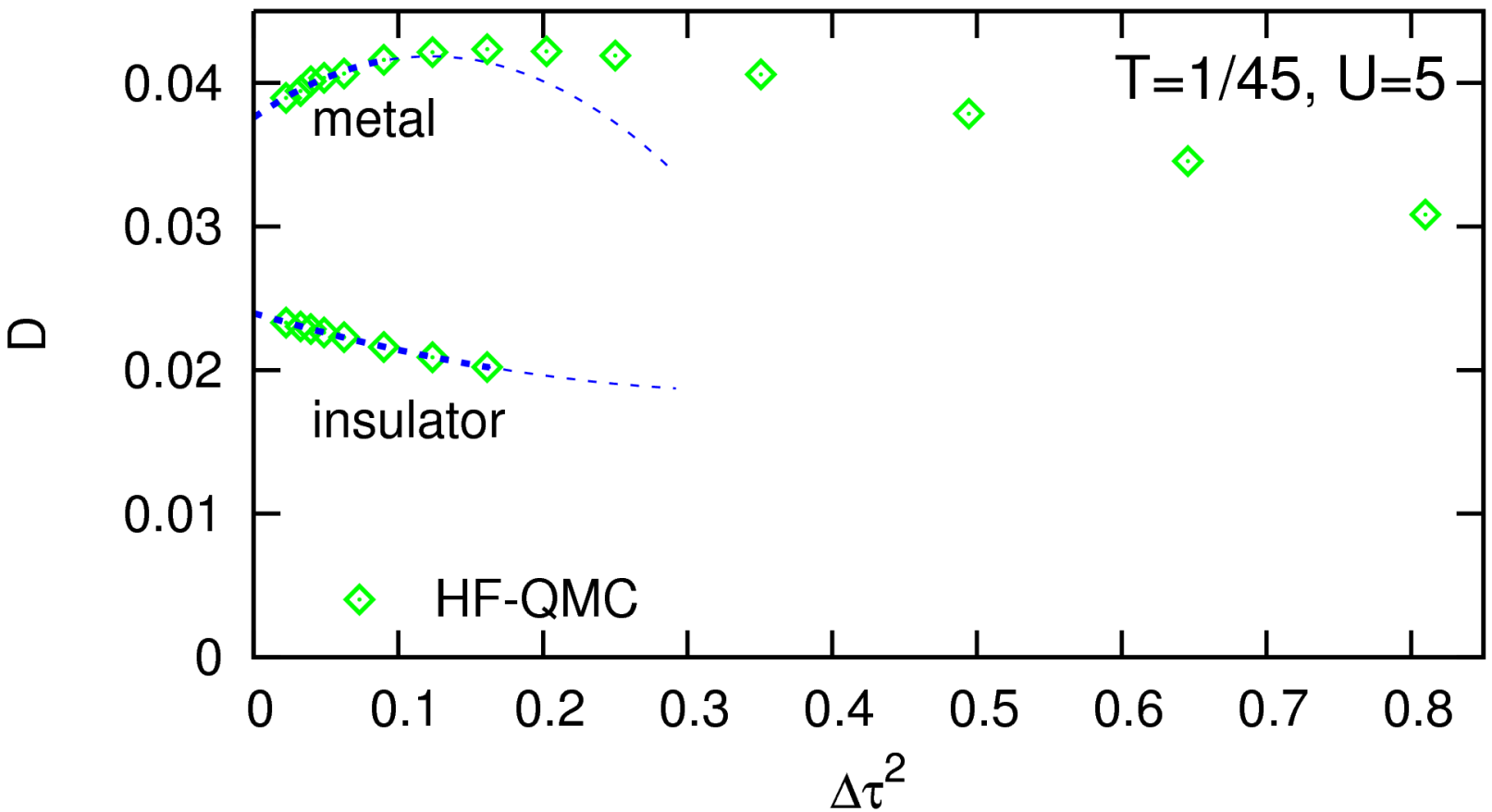

Conventional HF-QMC: no insulating solution for $\Delta\tau \gtrsim 0.4$

very irregular $\Delta\tau$ dependence beyond $\Delta\tau \approx 0.3$

Comparison: double occupancy $D = \langle n_{i\uparrow} n_{i\downarrow} \rangle$ near Mott transition

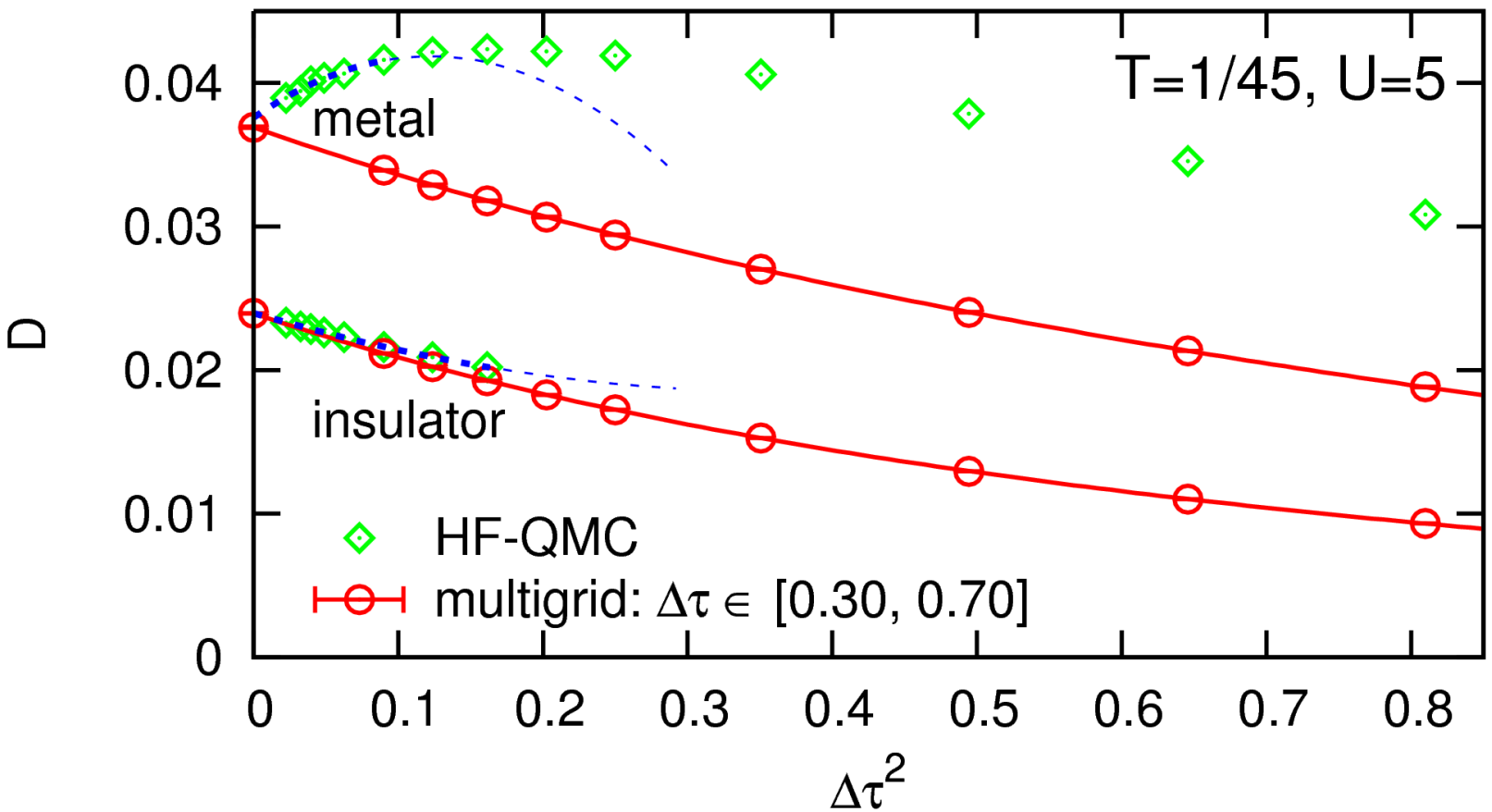

Conventional HF-QMC: no insulating solution for $\Delta\tau \gtrsim 0.4$

very irregular $\Delta\tau$ dependence beyond $\Delta\tau \approx 0.3$

Multigrid HF-QMC: vastly larger useful range of $\Delta\tau$

Systematic study: impact of grid range (on double occupancy)

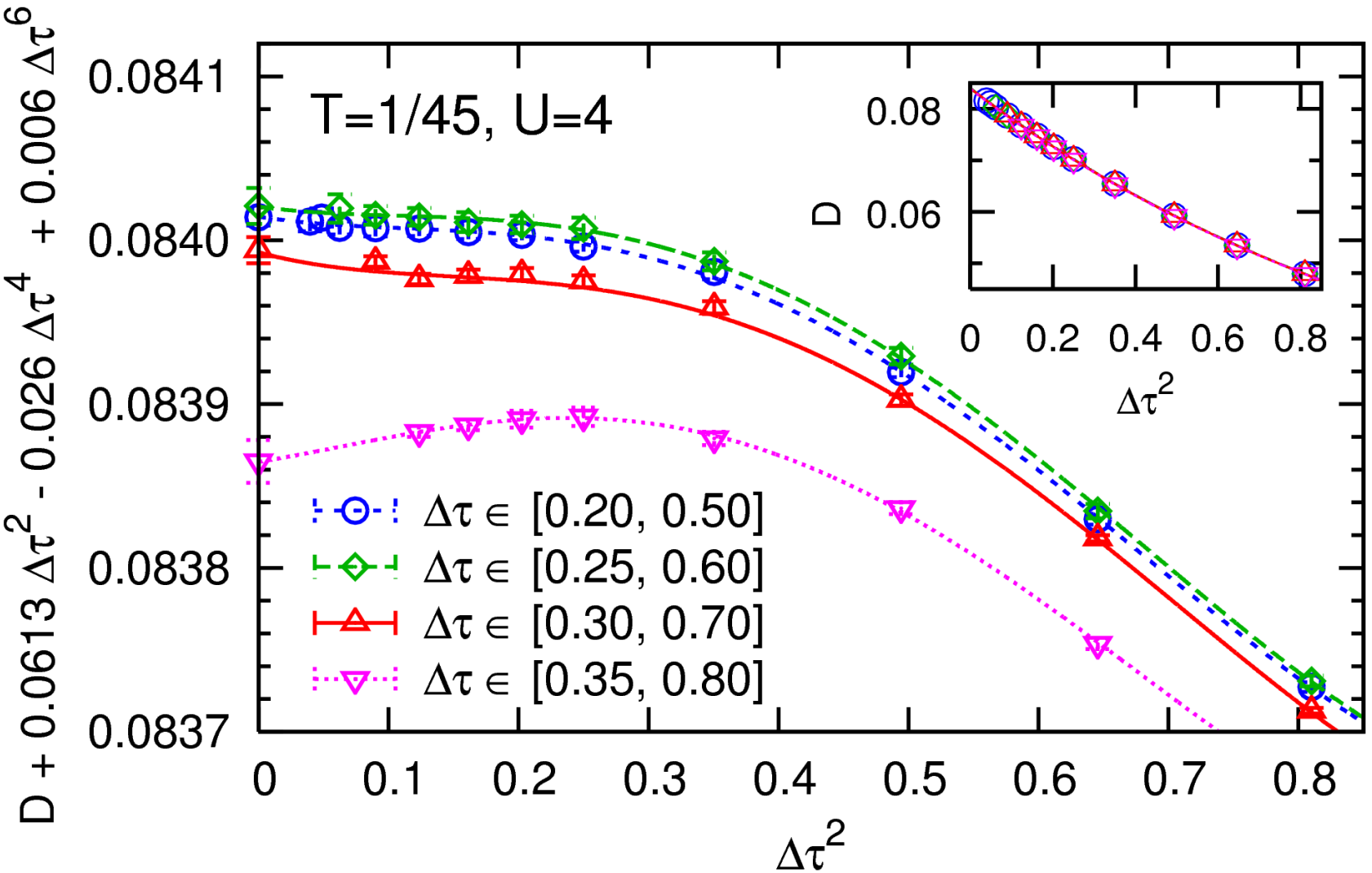

Multigrid HF-QMC usually "numerically exact" for $\tau_{\text{min}} \lesssim 0.3$

Efficiency: potential energy $E_{pot} = UD$ (at $U = W = 4$)

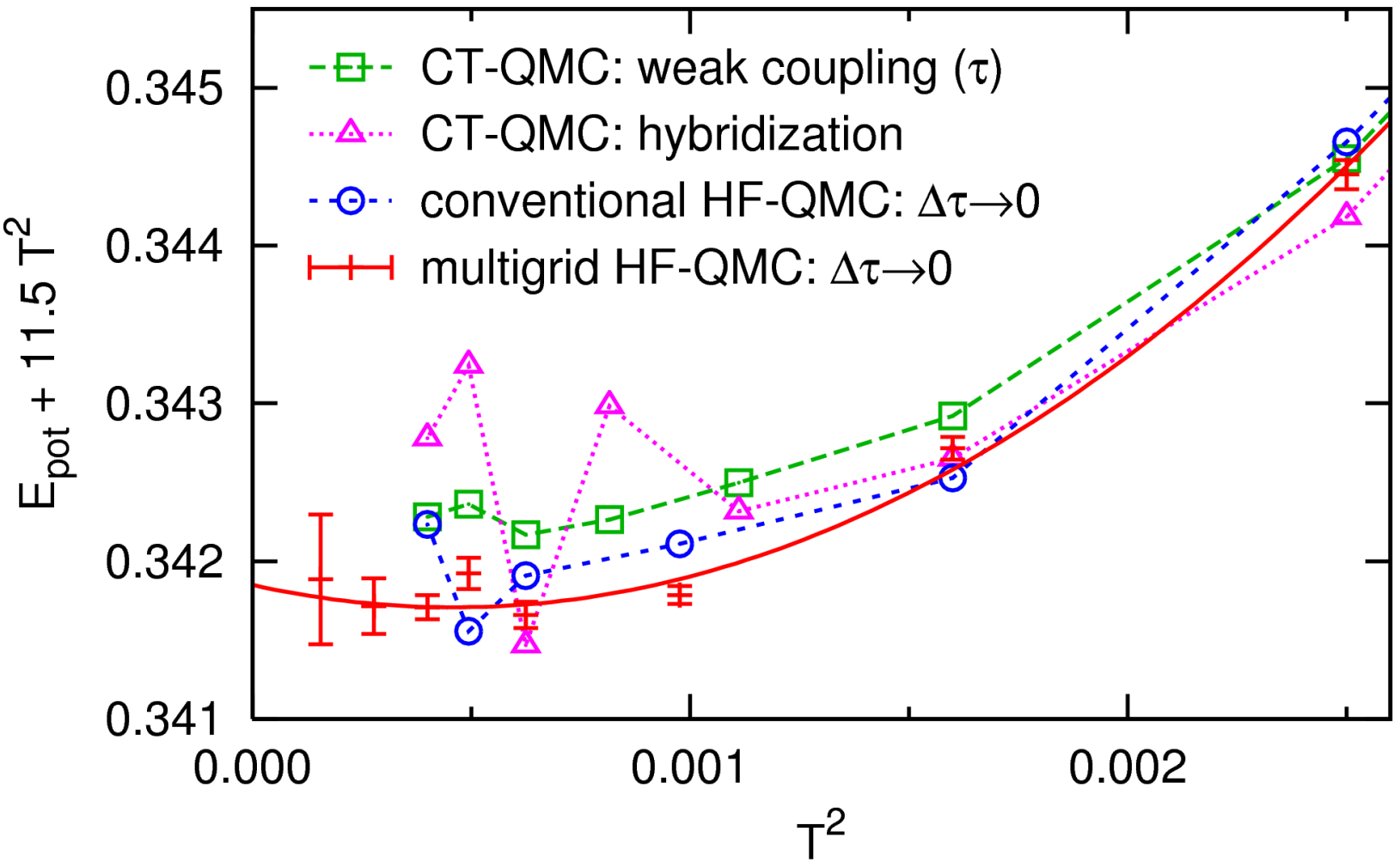

No more "difficult observables" for multigrid HF-QMC

Higher precision than CT-QMC methods at same effort

Spectral weight transfer at the Mott transition

Question: how does the Mott metal-insulator transition take place, precisely?

Spectral weight transfer at the Mott transition

Question: how does the Mott metal-insulator transition take place, precisely?

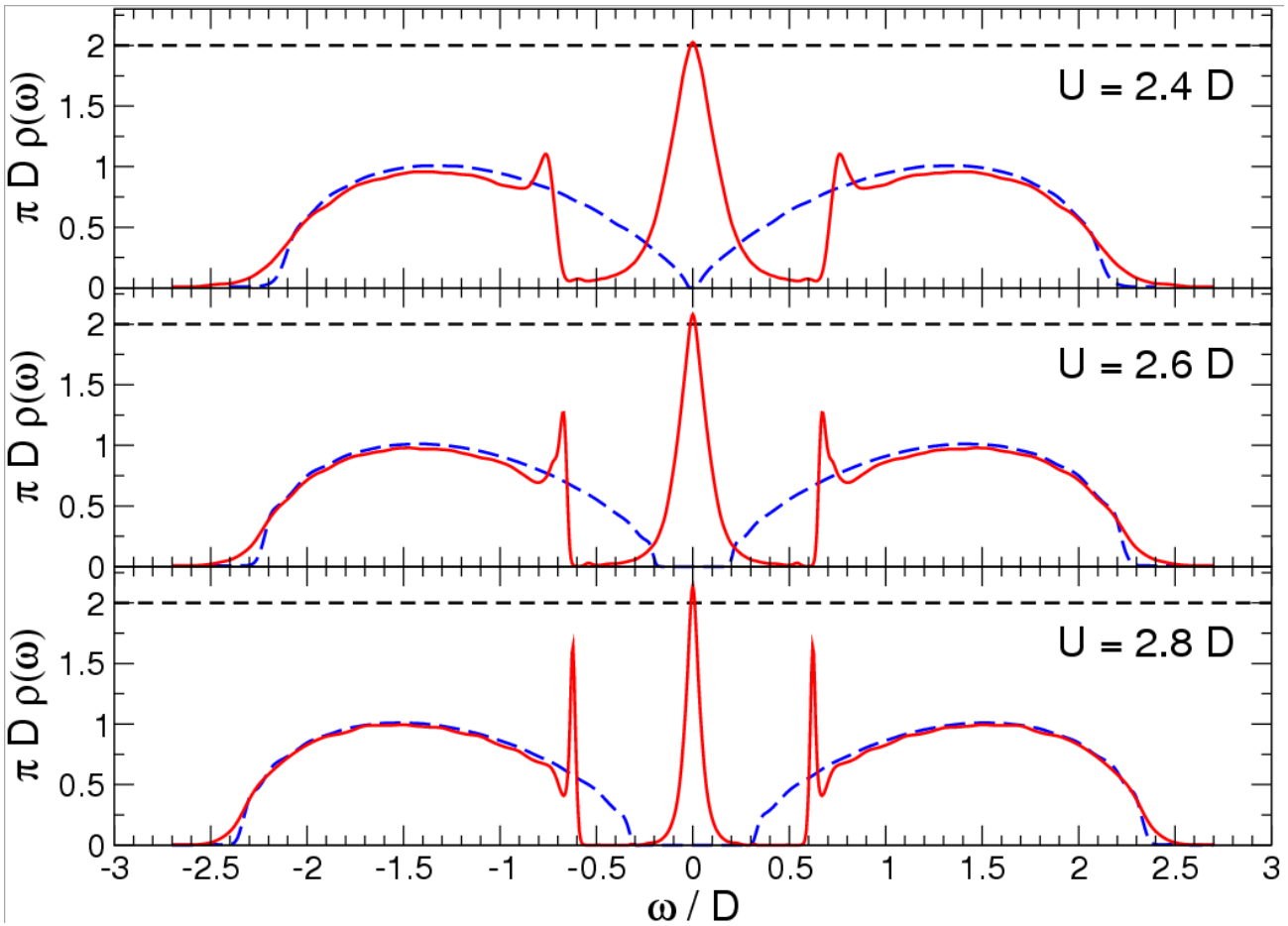

Dynamical DMRG $\rightsquigarrow$ Hubbard band subpeaks in metallic phase (at $T = 0$)

[Karski, Raas, Uhrig, PRB (2005)]

Spectral weight transfer at the Mott transition

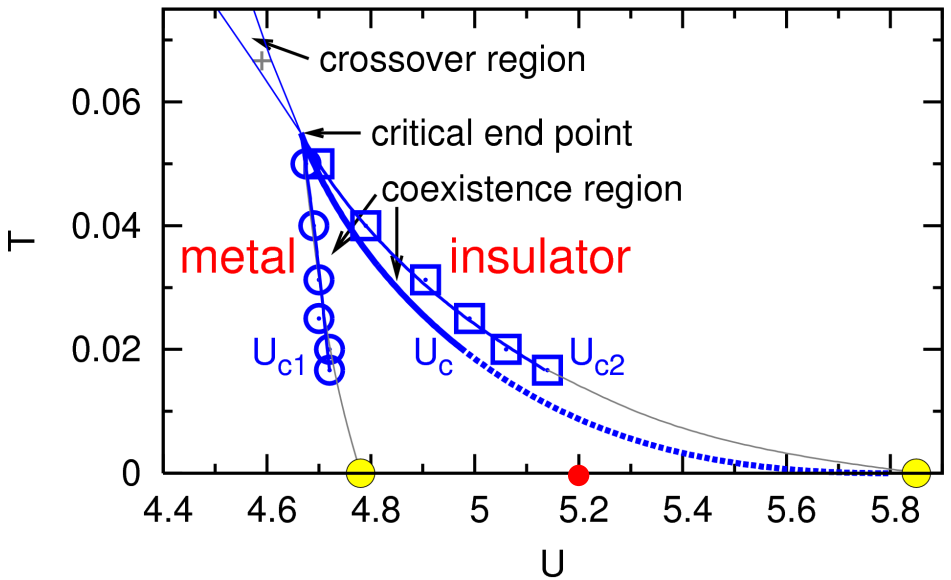

tor transition take place, precisely?

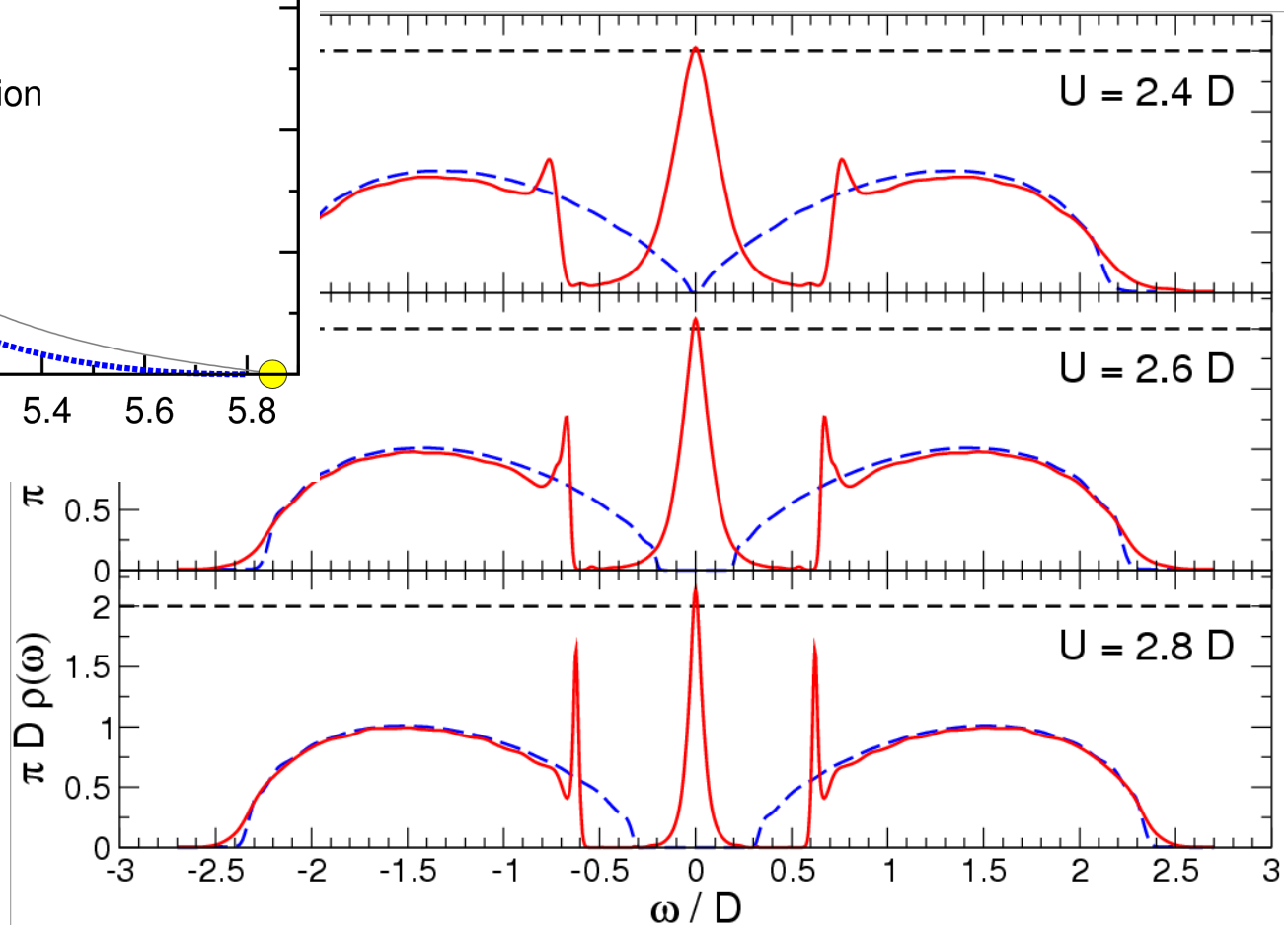

Dynamical DMRG $\rightsquigarrow$ Hubbard band subpeaks in metallic phase (at $T = 0$)

[Karski, Raas, Uhrig, PRB (2005)]

Spectral weight transfer at the Mott transition

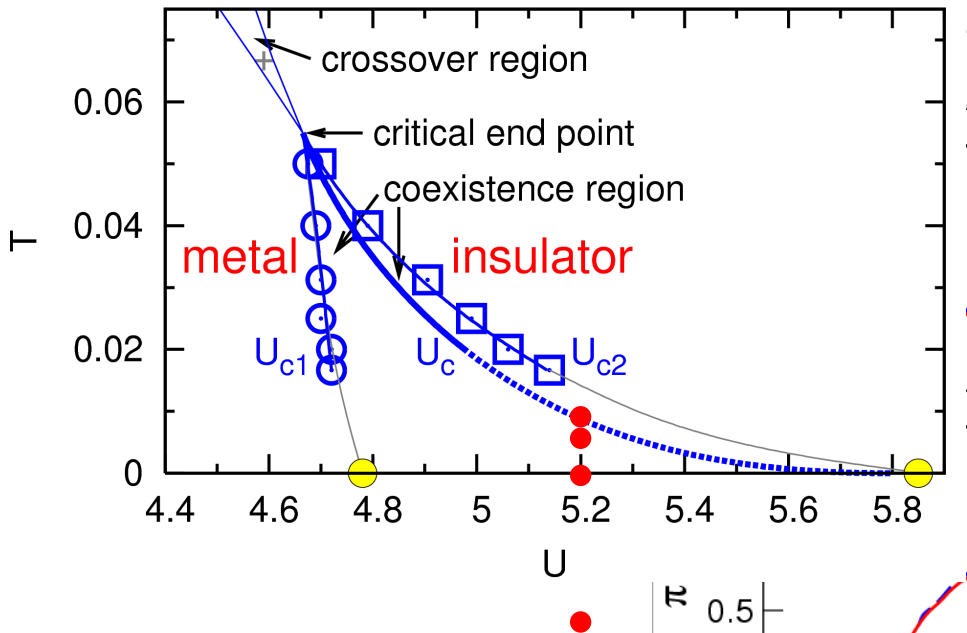

tor transition take place, precisely?

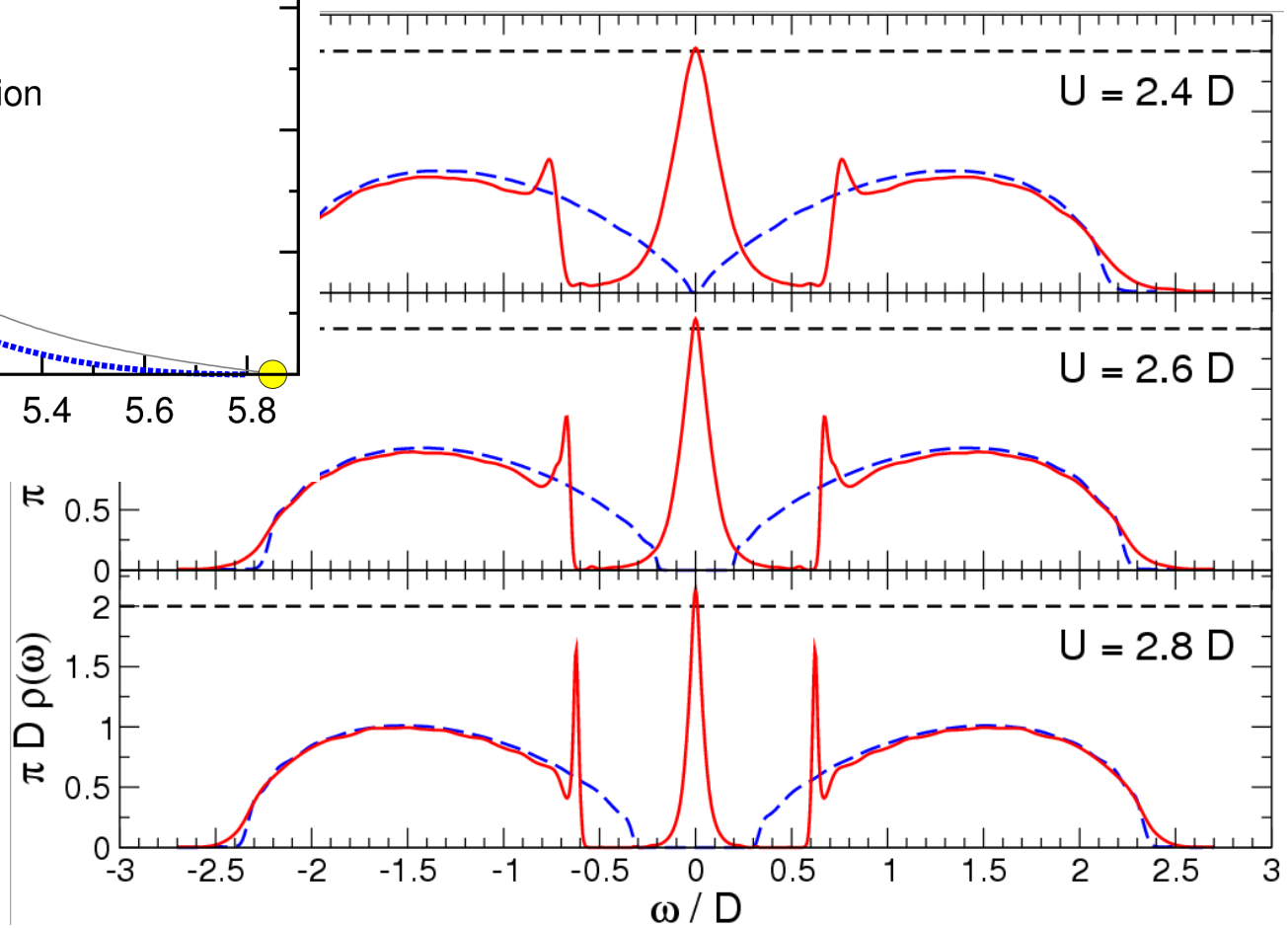

Dynamical DMRG $\rightsquigarrow$ Hubbard band subpeaks in metallic phase (at $T = 0$)

[Karski, Raas, Uhrig, PRB (2005)]

Verify using multigrid HF-QMC. . .

Analysis via difference of spectral functions (symmetric in ω) at $U = 5.2$

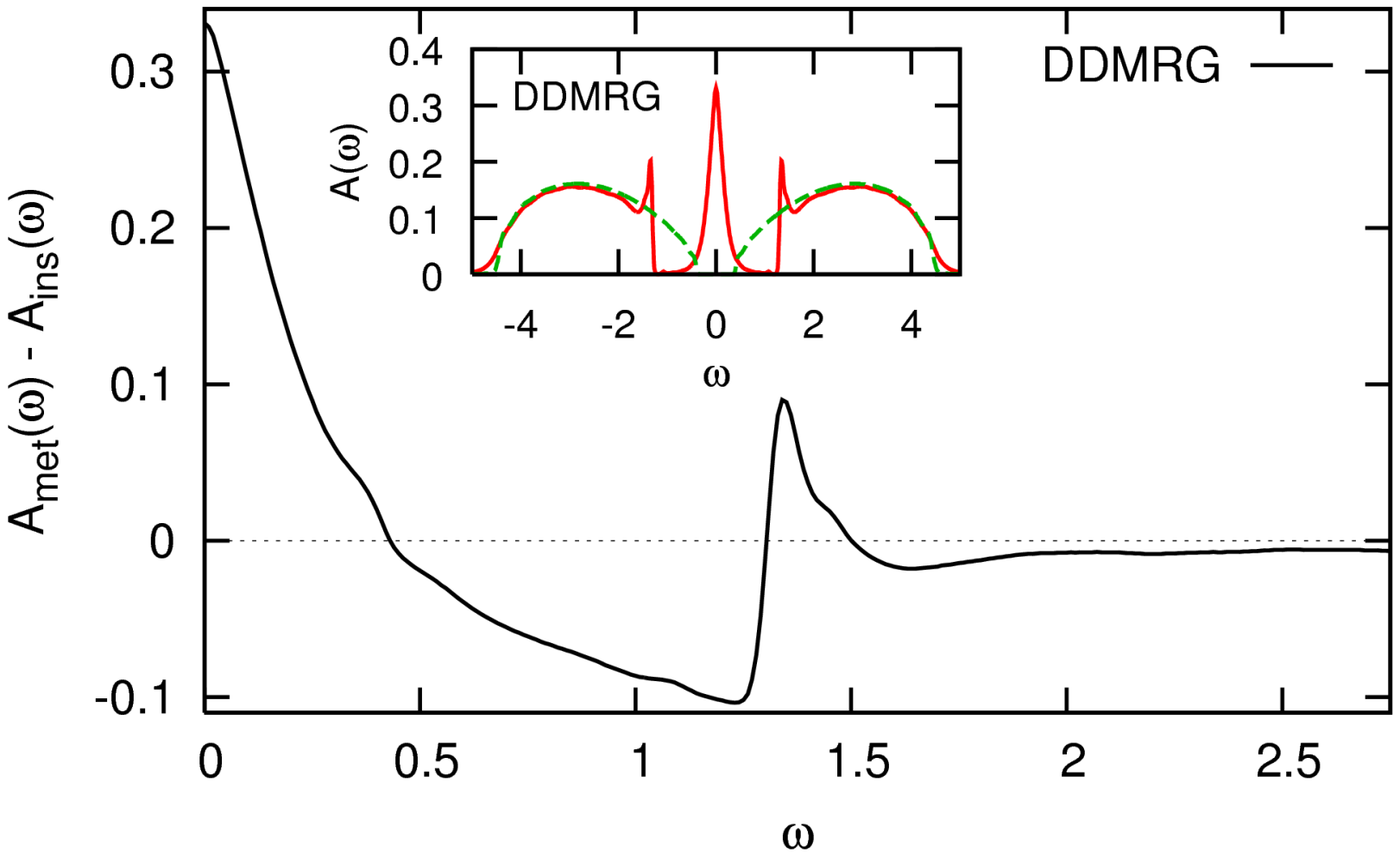

Problems for QMC: (i) analytic continuation of QMC data ill-conditioned

(ii) no $T \to 0$ extrapolation of spectra

Difference Green functions in imaginary time

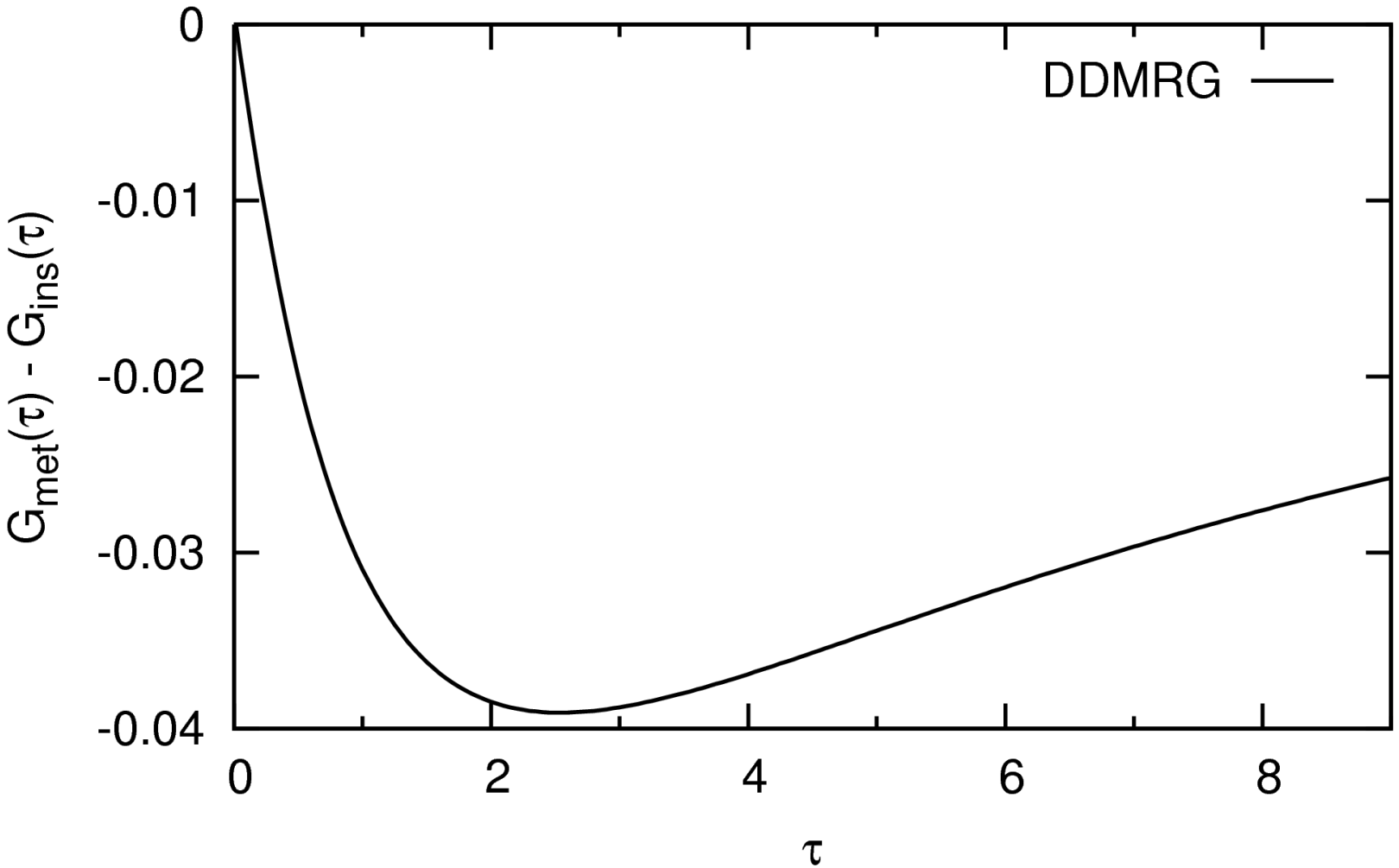

Difference Green functions in imaginary time

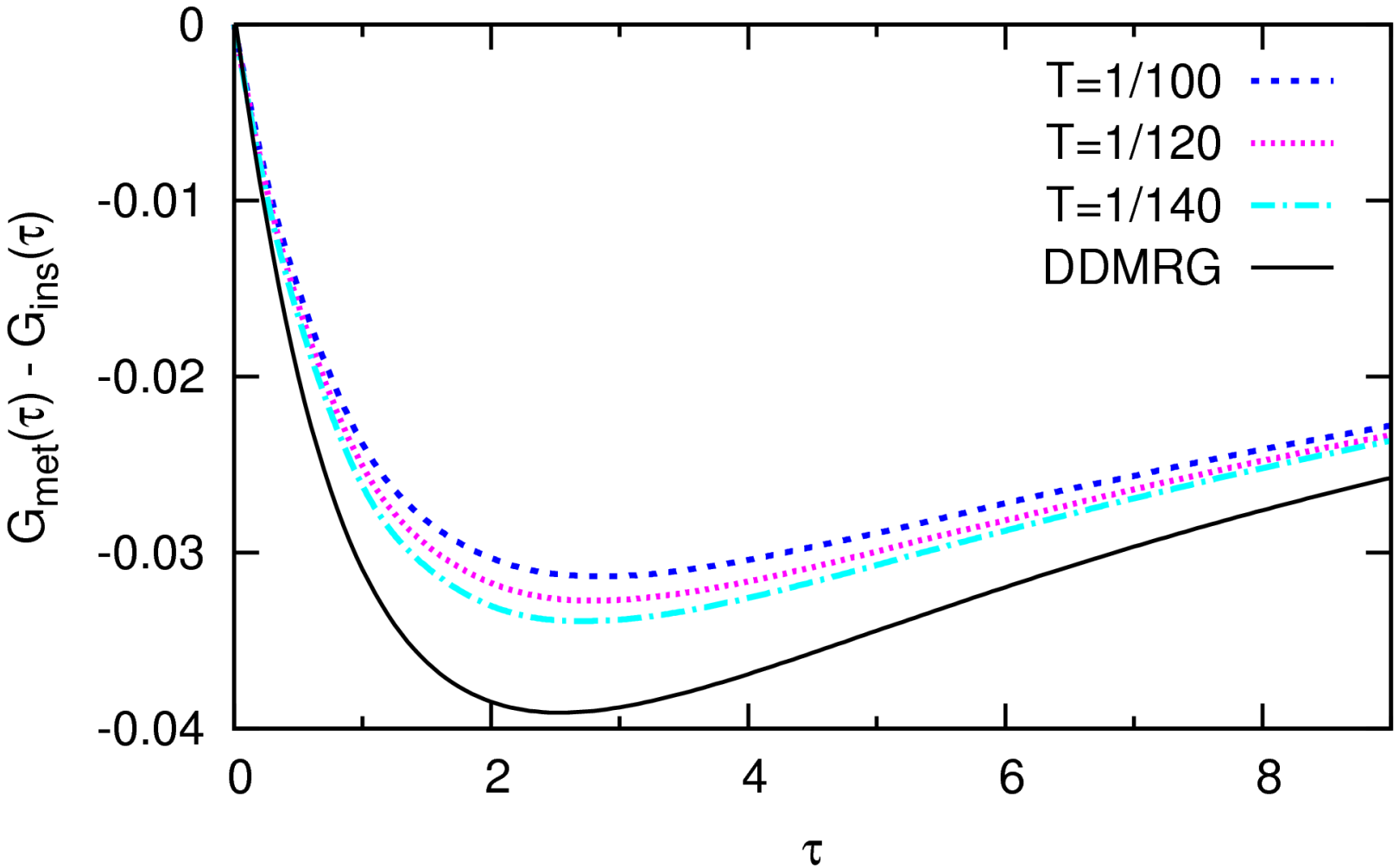

Difference Green functions in imaginary time

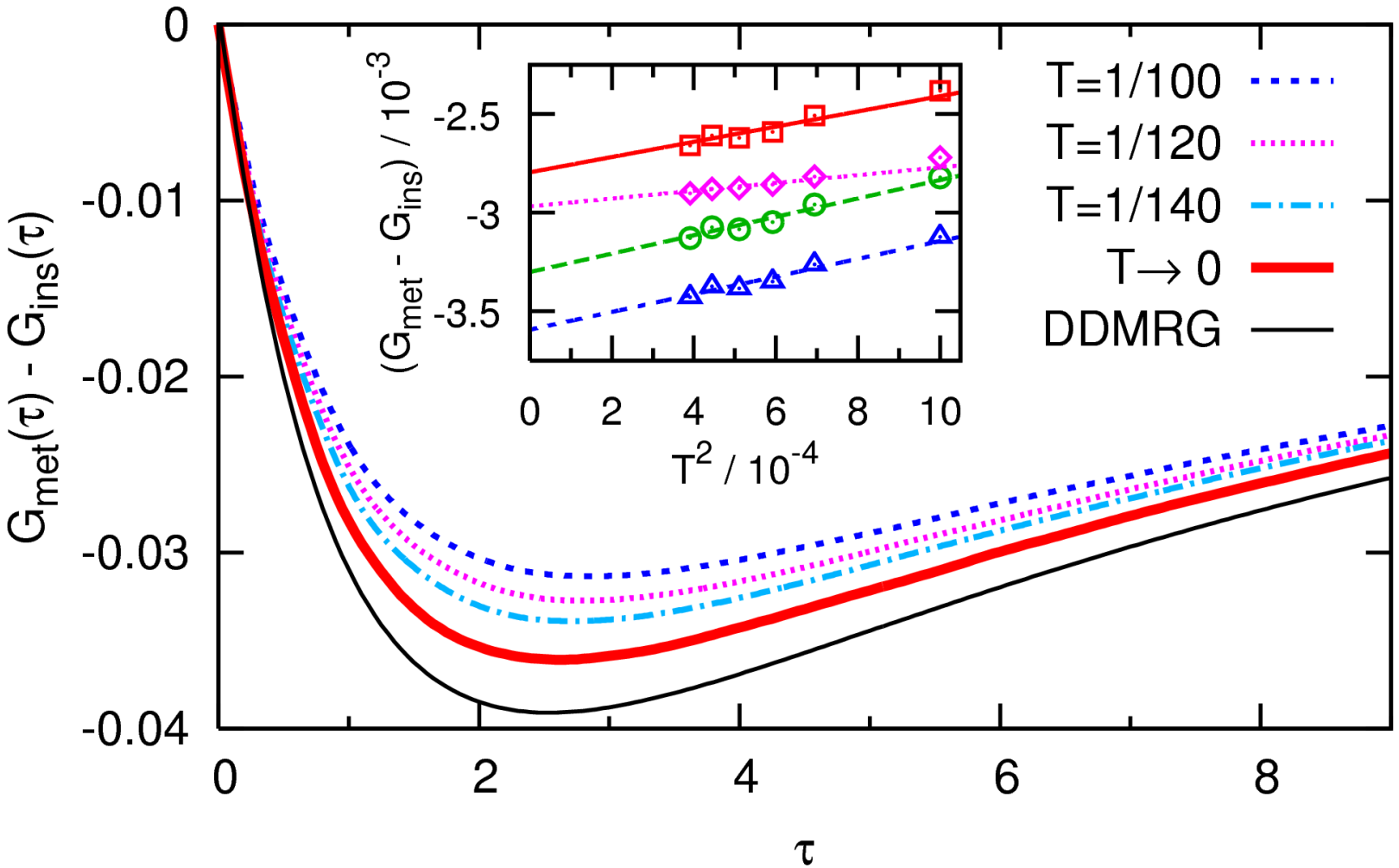

Multigrid HF-QMC data precise within linewidths [NB, arXiv:0801.1222]

DDMRG overestimates spectral weight transfer at $U = 5.2$ by about 10%!

Difference spectra

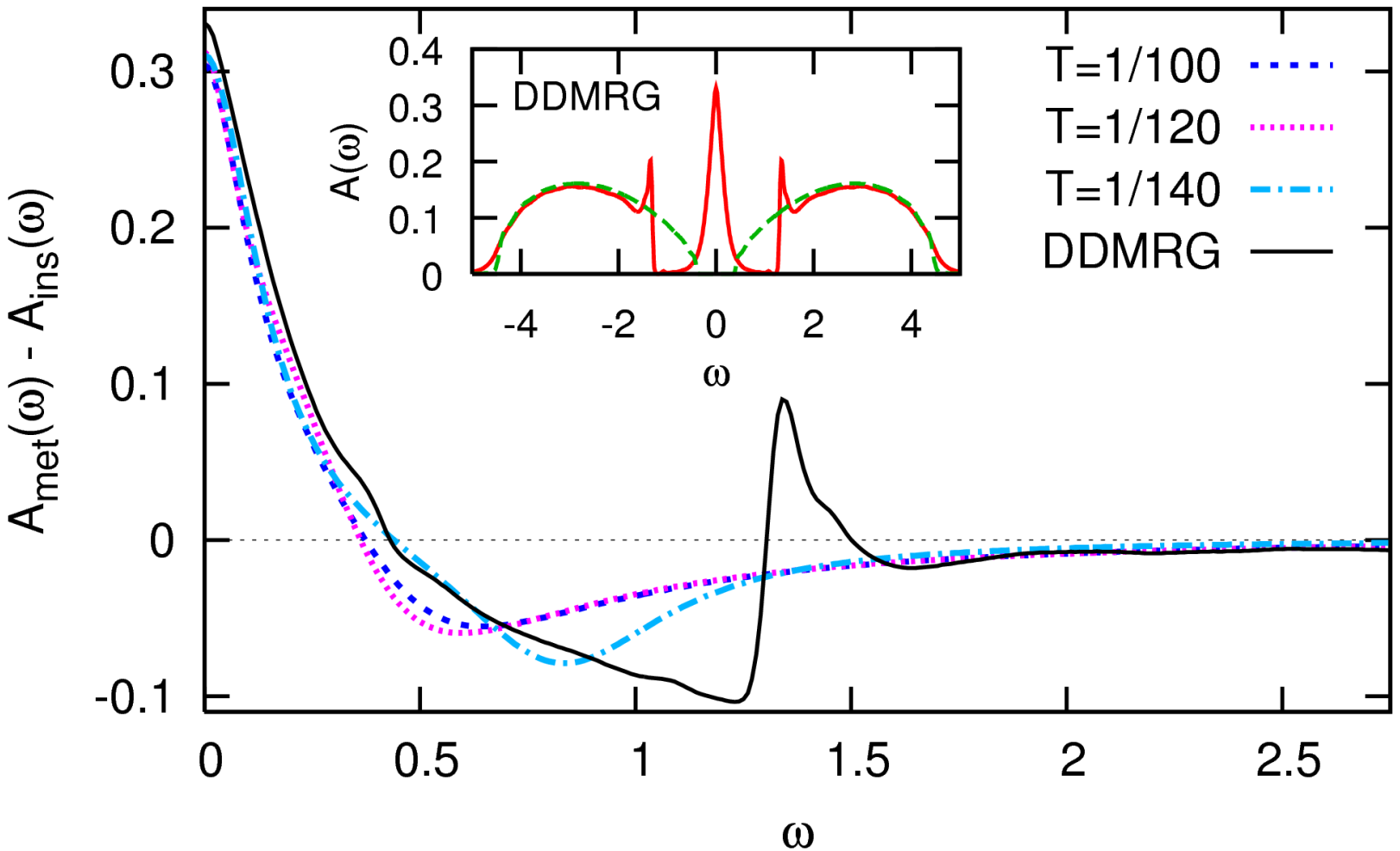

Similarities, but no indication for feature at $\omega = 1.3$ in QMC data

QMC spectral data via Padé interpolation, may be overly smooth [NB, arXiv:0801.1222]

Summary

Efficiency of QMC DMFT solvers: HF-QMC competitive (for not too low T)

Unbiased Green functions and spectra from HF-QMC

Multigrid Hirsch-Fye quantum Monte Carlo algorithm

- Quasi continuous time $\rightsquigarrow$ strictly "numerically exact"
- Stable and precise even at phase boundaries
- More efficient, lower T

Spectral weight transfer at the Mott transition

Summary

Efficiency of QMC DMFT solvers: HF-QMC competitive (for not too low T)

Unbiased Green functions and spectra from HF-QMC

Multigrid Hirsch-Fye quantum Monte Carlo algorithm

- Quasi continuous time $\rightsquigarrow$ strictly "numerically exact"
- Stable and precise even at phase boundaries
- More efficient, lower T

Spectral weight transfer at the Mott transition

Outlook

Breakdown of a Fermi liquid and low-T specific heat

Flavor-selective Mott transitions in ultracold quantum gases (SFB/TR 49)

Material-specific multiband calculations in context of LDA+DMFT

Summary

Efficiency of QMC DMFT solvers: HF-QMC competitive (for not too low T)

Unbiased Green functions and spectra from HF-QMC

Multigrid Hirsch-Fye quantum Monte Carlo algorithm

- Quasi continuous time $\rightsquigarrow$ strictly "numerically exact"
- Stable and precise even at phase boundaries
- More efficient, lower T

Spectral weight transfer at the Mott transition

Outlook

Breakdown of a Fermi liquid and low-T specific heat

Flavor-selective Mott transitions in ultracold quantum gases (SFB/TR 49)

Material-specific multiband calculations in context of LDA+DMFT

Significant extension of compute cluster . . .

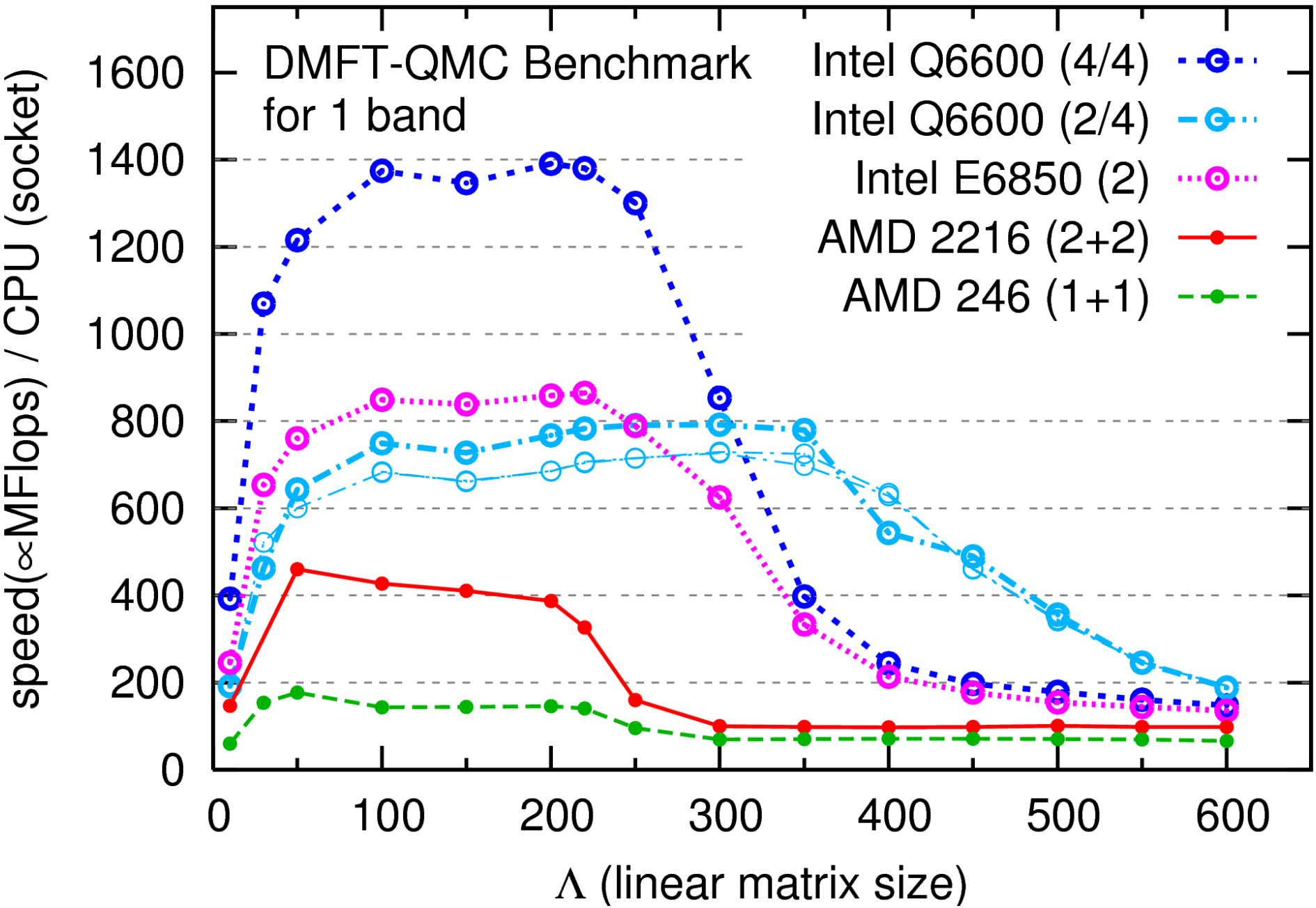
DMFT-QMC Benchmark
for 1 band
Intel Q6600 (4/4)
Intel Q6600 (2/4)
Intel E6850 (2)
AMD 2216 (2+2)
AMD 246 (1+1)
speed(∝MFlops) / CPU (socket)
Λ (linear matrix size)
0
200
400
600
800
1000
1200
1400
1600
0
100
200
300
400
500
600